

Chapter 4

Mathematical Model

A mathematical model of aircraft dynamics is required to study handling qualities. The mathematical models described in this chapter will be used to perform the following two functions:

- The calculation of the short period and phugoid mode properties of an aircraft, eg. the natural frequency and the damping ratio.
- The execution of flight simulations with which time domain responses for an aircraft are calculated.

The Exulans, Piper Cherokee, ASW-19 and the SB-13 mathematical models are presented in this chapter. The gust disturbance model used in time domain simulations is also presented.

4.1 Definition of Aircraft Axis System

A frame of reference is required for calculating the magnitudes of aircraft aerodynamic coefficients, aircraft positions and rotations. Axis systems that are frequently used in flight mechanics (Stevens & Lewis, 1992:62) were chosen for this purpose.

The axis systems that are used throughout this document are shown in Figure 4.1. This figure contains a gull-wing aircraft and the wind and body axis systems. Both are right handed axis systems. All rotations about an

axis are taken positive when they satisfy the right hand rule for rotations. The pitch rotations and attitude angles that are simulation outputs follow this convention.

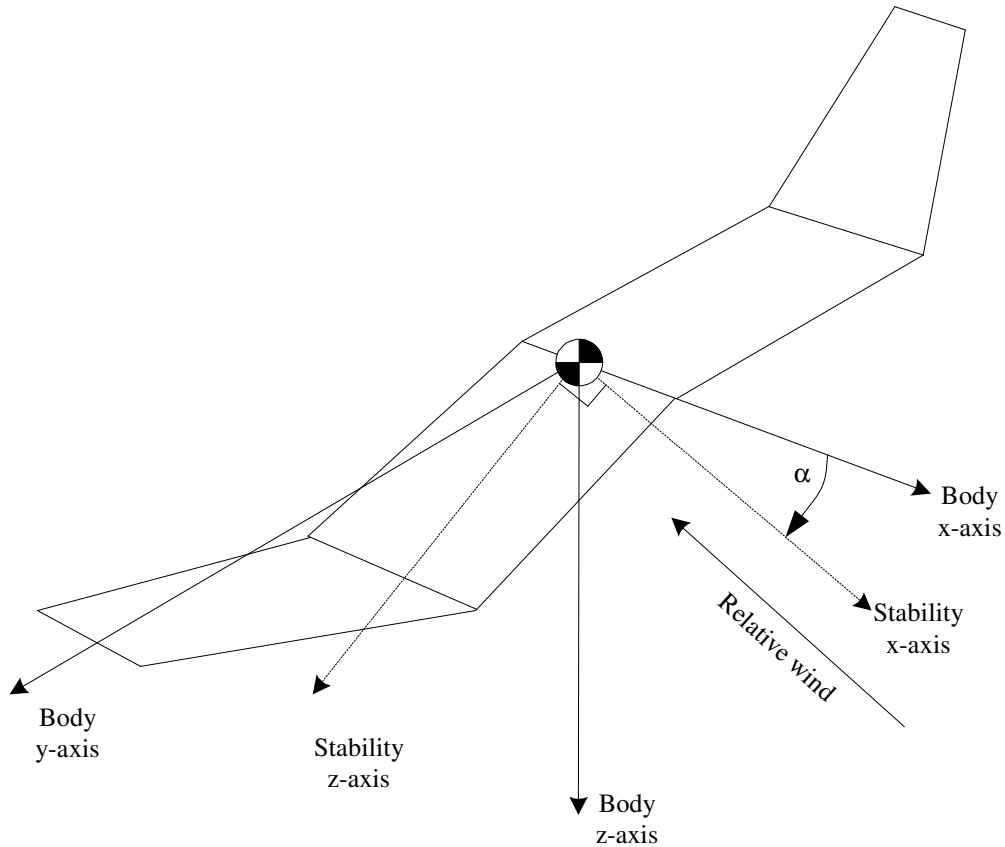


Figure 4.1: Aircraft axes system used in this document.

All aerodynamic coefficients used in this study are calculated in the wind axis system (stability axis system) with the *CG* as reference point. The body axis system is used internally by the simulation code used in this study.

4.2 Aircraft Model Characterisation

A simulation model requires aerodynamic coefficients and aircraft mass distribution data as input. The literature used to calculate these characteristics

for a typical aircraft is described here. This study contains model descriptions of four aircraft namely the Piper Cherokee, the ASW-19, the SB-13 and the Exulans.

Aerodynamic parameters such as the lift and moment curve slopes were obtained from vortex lattice methods.

Aerodynamic characteristics of the Exulans aircraft were also obtained from Crosby (2000). Mass distribution data of the Exulans aircraft was obtained from Huysen (2000). The aircraft inertia was calculated using the mass distribution data.

The methods presented in Abbot & von Doenhoff (1959) were used in some cases to provide estimates for overall lift of linearly tapered wings. This reference provides aerodynamic data for a wide variety of wing sections. It also provides checks for the effect of control surface deflections on overall lift and moment coefficients that are calculated by means of vortex lattice methods.

Aerodynamic data on the Piper Cherokee was obtained from McCormick (1995).

The wind tunnel data presented in Althaus & Wortmann (1981) was used to obtain the aerodynamic characteristics of the wing profiles of the ASW-19 aircraft.

Aerodynamic data on the airfoil sections of the SB-13 was obtained from Horstmann & Shürmeyer (1985).

Where no wind tunnel airfoil data was available, the XFOIL panel method was used to calculate the characteristics. (Drela & Youngren, 2000)

Stability derivatives, such as C_{Mq} are very important with respect to the modelling of tailless aircraft. According to the literature, four types of techniques are mostly used for estimating stability derivatives:

- wind tunnel results (Fremaux & Vairo, 1995)
- System identification using flight test results like the studies performed by Moes & Iliff (2002) and Browne (2003)
- Numerical methods such as Computational Fluid Dynamics or *CFD*

(Park, 2000) and Vortex Lattice methods or *VLMs* (Kuethe & Chow, 1998)).

- Manual calculation techniques based on empirical data (Roskam, 1971).

Experimental (wind tunnel) methods were not used to measure aerodynamic characteristics of the gull-wing configuration. This was avoided because the handling qualities of a general configuration was investigated in this study, as opposed to that of a final design. The different aerodynamic parameters influencing handling qualities have to be varied for such an investigation. The added value of accurately measured properties diminishes when a range of values are to be investigated. An additional consideration was that it is difficult to achieve acceptable dynamic similarity between small and full-scale models for the specific case of the Exulans. This is due to the geometry of the aircraft and the low true airspeed (maximum true airspeed is less than 110 km/h) for which it is designed.

System identification was not employed because a representative gull-wing aircraft was not available for flight testing at the time of completion of this study.

It was decided not to use *CFD* as part of this study since specialised expertise is necessary in creating models to perform analysis with sufficient accuracy.

Two Vortex Lattice Methods were used to calculate the stability derivatives of the aircraft that were modeled in this study. The two *VLM* implementations are Tornado (Melin, 2001) and JKVLM (Kay et al., 1996). Vortex Lattice Methods can accommodate complex aircraft geometry and require little computational effort. It has been shown (Kay et al., 1996) that methods such as JKVLM have produced results that give good correlation with wind tunnel data and DATCOM results. Toll & Queijo (1948) gives approximate relations for the stability derivatives for wings of different taper and sweepback. The calculations based on this source were used to check the Vortex Lattice Method results.

The methods of Roskam (1971) are based on empirical data and manual calculation techniques and were also used for estimating the magnitudes of

stability derivatives.

An example of how model characterisation is done for a tailless aircraft is presented in Ashkenas & Klyde (1989). The techniques presented in this reference was used in this study.

Nickel & Wohlfahrt (1994:468) provided some information on the performance of the SB-13, such as the optimum glide ratio.

Drag polar information as well as mass information of the ASW-19 was found on the internet (Anonymous, n.d. c).

4.3 Stability Derivatives

The stability derivatives will be used to create the aircraft mathematical model. These parameters are defined using the axis system defined in Section 4.1.

Many aerodynamic coefficients are approximately constant or vary in an approximately linear way over a range of angles of attack. This is advantageous since this fact can be used to simplify the aircraft mathematical model. The stability derivatives are simply the gradients of aerodynamic coefficients with respect to an angle (e.g. angle of attack, α).

The stability derivatives have their origins from the linear small perturbation equations (Bryan, 1911).

The stability derivatives for motion in the pitch plane are shown in Table 4.1.

Table 4.1: Longitudinal dimensional and dimensionless derivatives (Stevens & Lewis, 1992:105).

$X_V = -\frac{\bar{q}S}{mV_T}(2C_D + C_{D_V})$	$C_{D_V} \equiv V_T \frac{\partial C_D}{\partial V_T}$
$X_\alpha = \frac{\bar{q}S}{m}(C_L - C_{D_\alpha})$	$C_{D_\alpha} \equiv \frac{\partial C_D}{\partial \alpha}$
$X_{\delta_e} = -\frac{\bar{q}S}{m}C_{D_{\delta_e}}$	$C_{D_{\delta_e}} \equiv \frac{\partial C_D}{\partial \delta_e}$
$Z_V = -\frac{\bar{q}S}{mV_T}(C_D + C_{L_V})$	$C_{L_V} \equiv V_T \frac{\partial C_L}{\partial V_T}$
$Z_\alpha = -\frac{\bar{q}S}{m}(C_D + C_{L_\alpha})$	$C_{L_\alpha} \equiv \frac{\partial C_L}{\partial \alpha}$
$Z_{\dot{\alpha}} = -\frac{\bar{q}S\bar{c}}{2mV_T}C_{L_{\dot{\alpha}}}$	$C_{L_{\dot{\alpha}}} \equiv \frac{2V_T}{\bar{c}} \frac{\partial C_L}{\partial \dot{\alpha}}$
$Z_q = -\frac{\bar{q}S\bar{c}}{2mV_T}C_{L_q}$	$C_{L_q} \equiv \frac{2V_T}{\bar{c}} \frac{\partial C_L}{\partial q}$
$Z_{\delta_e} = -\frac{\bar{q}S}{m}C_{L_{\delta_e}}$	$C_{L_{\delta_e}} \equiv \frac{\partial C_L}{\partial \delta_e}$
$M_v = \frac{\bar{q}S\bar{c}}{I_{yy}V_T}(2C_M + C_{M_V})$	$C_{M_V} \equiv V_T \frac{\partial C_M}{\partial V_T}$
$M_\alpha = \frac{\bar{q}S\bar{c}}{I_{yy}}C_{M_\alpha}$	$C_{M_\alpha} \equiv \frac{\partial C_M}{\partial \alpha}$
$M_{\dot{\alpha}} = \frac{\bar{q}S\bar{c}}{I_{yy}} \frac{\bar{c}}{2V_T}C_{M_{\dot{\alpha}}}$	$C_{M_{\dot{\alpha}}} \equiv \frac{2V_T}{\bar{c}} \frac{\partial C_M}{\partial \dot{\alpha}}$
$M_q = \frac{\bar{q}S\bar{c}}{I_{yy}} \frac{\bar{c}}{2V_T}C_{M_q}$	$C_{M_q} \equiv \frac{2V_T}{\bar{c}} \frac{\partial C_M}{\partial q}$
$M_{\delta_e} = \frac{\bar{q}S\bar{c}}{I_{yy}}C_{M_{\delta_e}}$	$C_{M_{\delta_e}} \equiv \frac{\partial C_M}{\partial \delta_e}$

4.4 Equations of Motion

The equations of motion of the mathematical model are shown in Equation 4.1. The equations are presented in a state space format. These equations are a set of differential equations that may be solved with a suitable numerical integration method in order to calculate time domain responses.

The state space representation of the equations of motion presented here (Equation 4.1) is based on Equations 2.4-23 to 2.4-26 (Stevens & Lewis, 1992:88-89). Similar equations of motion are presented in the work of Etkin (1972).

$$\dot{\mathbf{x}} = \begin{bmatrix} \dot{V}_T \\ \dot{\alpha} \\ \dot{\theta} \\ \dot{q} \end{bmatrix} = \begin{bmatrix} \frac{-\frac{1}{2}\rho V_T^2 S C_D}{m} - g \sin(\theta - \alpha) \\ \frac{-\frac{1}{2}\rho V_T^2 S C_L + m(V_T q + g \cos(\theta - \alpha))}{m V_T} \\ q \\ \frac{\frac{1}{2}\rho V_T^2 S \bar{c} (C_M + \frac{\frac{1}{2}\bar{c} C_{Mq} q}{V_T})}{I_{yy}} \end{bmatrix} + \begin{bmatrix} \frac{-\frac{1}{2}\rho V_T^2 S C_{D\delta_e} \cdot \delta_e}{m} \\ \frac{-\frac{1}{2}\rho V_T^2 S C_{L\delta_e} \cdot \delta_e}{m V_T} + q_g \\ 0 \\ \frac{\frac{1}{2}\rho V_T^2 S \bar{c} (C_{M\delta_e} \cdot \delta_e + \frac{\frac{1}{2}\bar{c} C_{Mq} q_g}{V_T})}{I_{yy}} \end{bmatrix} \quad (4.1)$$

4.5 Analytical Approximations for Short Period and Phugoid Modes

The damping ratios and natural frequencies of the short period and phugoid longitudinal modes were used to evaluate the flying qualities of three different aircraft. The aircraft models were required to have a sufficient level of model accuracy in order to calculate the natural frequencies and damping ratios.

Analytical approximations for both the short period and phugoid modes were used to identify the parameters that have the largest effect on the accuracy of the natural frequency and damping ratio calculation. From the approximations it was possible to determine which parameters have the most significant influence of the natural frequencies and damping ratios. The analytical approximation equations were obtained from Stevens & Lewis (1992:206-210).

4.5.1 The Short Period Approximation

An expression for the natural frequency of the short period mode is presented in Equation 4.2 and an expression for the damping ratio is presented in Equation 4.3.

C_D is a parameter of $\omega_{n_{sp}}$ (see Equation 4.2). The equilibrium drag coefficient is normally much smaller than the lift curve slope and therefore its influence on the frequency is less significant than the other parameters.

It is clear from the $\omega_{n_{sp}}$ equation that C_{M_q} and C_{M_α} are important parameters with respect to natural frequency.

In the case of a light weight aircraft, the contribution of pitch stiffness (C_{M_α}) to $\omega_{n_{sp}}$ becomes less significant than that of (C_{M_q}).

The mass moment of inertia around the Y-Y axis of the aircraft is a very important parameter in the natural frequency and the damping ratio. When the inertia is large, $\omega_{n_{sp}}$ becomes smaller.

$$\omega_{n_{sp}} = \frac{1}{2} \rho V_T S \bar{c} \left[\frac{-C_{M_q}(C_D + C_{L_\alpha}) - (4m/\rho S \bar{c} C_{M_\alpha})}{2mI_{yy}} \right]^{\frac{1}{2}} \quad (4.2)$$

Pitch damping (C_{M_q}) and the damping effect of the empennage ($C_{M_{\dot{\alpha}}}$) are important parameters of the short period damping ratio. The damping ratio increases in magnitude as C_{M_q} and $C_{M_{\dot{\alpha}}}$ increases. The short period damping ratio decreases as inertia increases.

$$\zeta_{sp} = \frac{-\bar{c} \left[\frac{m}{I_{yy}} \right]^{\frac{1}{2}} \frac{C_{M_q} + C_{M_{\dot{\alpha}}} - 2I_{yy}(C_D + C_{L_{\dot{\alpha}}})/(\bar{c}^2 m)}{\left[-\frac{1}{2}C_{M_q}(C_D + C_{L_{\dot{\alpha}}}) - 2mC_{M_{\dot{\alpha}}}/(\rho S \bar{c}) \right]^{1/2}}}{4} \quad (4.3)$$

4.5.2 The Phugoid Approximation

The analytical approximation for the phugoid mode natural frequency is shown in the following equation:

$$\frac{\omega_{np}^2}{g} = \frac{(C_D + C_{L_{\dot{\alpha}}})(2C_M + C_{M_V}) - C_{M_{\dot{\alpha}}}(2C_L + C_{L_V})}{-\frac{1}{2}\bar{c}C_{M_q}(C_D + C_{L_{\dot{\alpha}}}) - C_{M_{\dot{\alpha}}}[mV_T^2/(\bar{q}S) - \frac{1}{2}\bar{c}C_{L_q}]} \quad (4.4)$$

The above equation can be simplified with some assumptions. This simplification is described in Stevens & Lewis (1992:209) and shortly summarised in the following paragraphs, as it is important to understand the relative importance of the different parameters of the equation.

The derivation of Equation 4.4 assumes that the engine (if the aircraft has one) thrust vector passes through the centre of gravity, in order that the equilibrium aerodynamic pitching moment is zero.

The natural frequency is a function of a number of parameters, one of which is the drag coefficient. Under most circumstances C_D is small in comparison with $C_{L_{\dot{\alpha}}}$. Let us assume (for the sake of simplification) that $C_D \ll C_{L_{\dot{\alpha}}}$. Also take into account that $C_M \approx 0$ at a trim flight condition. When the C_{M_V} , C_{L_V} and C_{L_q} coefficients are neglected (the magnitude of these coefficients are small close to a trim condition and small relative to other contributions), Equation 4.4 can be simplified as follows:

$$\frac{\omega_{np}^2}{g} = \frac{2C_{m_{\dot{\alpha}}}C_L}{\frac{1}{2}\bar{c}C_{m_q}C_{L_{\dot{\alpha}}} + 2mC_{m_{\dot{\alpha}}}/(\rho S)} \quad (4.5)$$

This equation shows that the phugoid natural frequency is proportional to the square root of the lift coefficient when the other derivatives in the

equation are constant. Inspection of Equation 4.5 also shows that the phugoid mode natural frequency decreases as damping (C_{M_q}) increases.

The analytical approximation for the phugoid damping ratio is presented in Equation 4.6. This expression is not very accurate Stevens & Lewis (1992:210), but is shown as a matter of completeness.

$$2\zeta_p\omega_{n_p} = \frac{-(X_V + X_{T_V}\cos\alpha_e + X_\alpha[M_q(Z_V - X_{T_V}\sin\alpha_e) - (V_T + Z_q)(M_V + M_{T_V})])}{M_qZ_\alpha - M_\alpha(V_T + Z_q)} \quad (4.6)$$

4.5.3 Tailed aircraft Sensitivity Analysis

A sensitivity analysis was used to explore the effects of aircraft parameters on natural frequency and damping ratio. The analytical approximations of natural frequency and damping ratio were used for the sensitivity study.

The properties of the aircraft modes of a Piper Cherokee aircraft were calculated in the sensitivity study. It was assumed that the aircraft is travelling at a fixed height and speed.

The damping ratio and natural frequency of the short period is calculated for the baseline configuration of the aircraft. The different parameters of the equations of these properties are then varied by 5% above and below the baseline. The effect of these changes on natural frequency and damping ratio are then calculated. Equations 4.2 and 4.3 were used to calculate short period natural frequency and damping ratio. The results of the study are presented in Table 4.2. The same analysis was performed on the phugoid natural frequency (using Equation 4.4) and the results are presented in Table 4.3.

This analysis was used as a precursor to the one presented in Chapter 5 and was used to select the parameters for the sensitivity study.

The analysis was performed for a density altitude of 1524m (5000ft) and a speed of 161km/h (100mph). The analysis was done for power-off gliding flight at a static margin of 23.75% and a 2.2° angle of attack.

The following conclusions were drawn:

- Air density (ρ), true airspeed (V_T), pitch moment of inertia (I_{yy}) and

the pitch stiffness (C_{M_α}) (and hence the static margin) have a large effect on short period natural frequency.

- The aerodynamic damping coefficient (C_{M_q}) has a large influence on the aircraft short period damping ratio. The damping effect due to the interaction between the main lifting surface and the horizontal tail ($C_{M_{\dot{\alpha}}}$) has an effect on the aircraft short period damping ratio, but its effect is smaller than that of the aerodynamic damping coefficient. Air density (ρ), the pitch moment of inertia (I_{yy}) and the pitch stiffness (C_{M_α}) also have a large influence on the damping ratio of the short period mode.
- The phugoid natural frequency is influenced by air density (ρ), the lift curve slope (C_{L_α}), aircraft mass (m) and pitch stiffness (C_{M_α}). These parameters influence the phugoid natural frequency because this mode involves an exchange in potential energy with kinetic energy.

It is important to note that C_{M_0} , C_{L_0} and $C_{M_{\delta_e}}$ are not very important parameters in the natural frequencies or the damping ratios of either of the aircraft dynamic modes. These quantities are more important with respect to the trim attitude. The $C_{M_{\delta_e}}$ variable also determines the control gain of the aircraft in the pitch plane.

Table 4.2: Results of the sensitivity analysis of the short period mode. (The absolute values of the changes in magnitude of the properties are shown)

Parameter	% change	$ \% \Delta \omega_{n_{sp}} $	$ \% \Delta \zeta_{sp} $
ρ	+5%	2.48%	2.45%
ρ	-5%	2.55%	2.52%
V_T	+5%	5.00%	0.00%
V_T	-5%	5.00%	0.00%
C_{M_q}	+5%	0.015%	3.622%
C_{M_q}	-5%	0.015%	3.623%
C_D	+5%	0.000%	0.001%
C_D	-5%	0.000%	0.001%
C_{L_α}	+5%	0.015%	0.015%
C_{L_α}	-5%	0.015%	0.015%
m	+5%	0.014%	0.062%
m	-5%	0.014%	0.069%
I_{yy}	+5%	2.41%	2.41%
I_{yy}	-5%	2.60%	2.60%
C_{M_α}	+5%	2.45%	2.40%
C_{M_α}	-5%	2.52%	2.58%
$C_{M_{\dot{\alpha}}}$	+5%	0.00%	1.28%
$C_{M_{\dot{\alpha}}}$	-5%	0.00%	1.28%

Table 4.3: Results of the sensitivity analysis of the phugoid mode. (The absolute values of the changes in magnitude of the properties are shown)

Parameter	% change	$ \% \Delta \omega_{np} $
ρ	+5%	2.45%
ρ	-5%	2.52%
C_{M_q}	+5%	0.015%
C_{M_q}	-5%	0.015%
C_D	+5%	0.015%
C_D	-5%	0.015%
C_{L_α}	+5%	1.810%
C_{L_α}	-5%	1.844%
m	+5%	2.396%
m	-5%	2.582%
I_{yy}	+5%	0.00%
I_{yy}	-5%	0.00%
C_{M_α}	+5%	1.78%
C_{M_α}	-5%	1.93%
$C_{M_{\dot{\alpha}}}$	+5%	0.00%
$C_{M_{\dot{\alpha}}}$	-5%	0.00%

4.6 Aircraft Mathematical Models

The mathematical model parameter values for the aircraft used in this study are listed in Table 4.4.

The following four aircraft types are used for a comparative handling characteristics analysis (see Section 6.2) with the gull-wing configuration:

- Piper Cherokee PA-28-180 - This aircraft is used because all the parameter values could be obtained from published data (McCormick, 1995). This model was also used for benchmarking of the simulation code. The aircraft is representative of a conventional powered aircraft.
- The ASW-19 standard glider - This aircraft is representative of a standard glider known to have very good handling qualities.
- The Akaflieg SB-13 Arcus sailplane - This aircraft is representative of a tailless glider, that has good flying qualities, except in turbulent conditions.
- The Exulans gull-wing configuration - The subject of the handling quality evaluation. Table 4.4 shows the mathematical model parameter values for an aircraft with the outboard wing sections swept back at 30° .¹ The sweep case presented in the table has a 10.7% static margin at the 30° sweep angle.

The planforms of these aircraft are shown in Appendix C.

All the coefficients relating to aircraft moments in Table 4.4 use the aircraft centre of gravity as the reference point. This convention will be followed throughout this document.

The gull-wing aircraft (Exulans) has low damping and pitch inertia when compared to aircraft with horizontal stabilisers. The values are low when compared to another tailless aircraft such as the SB-13. The difference between the SB-13 and gull-wing configuration is that the SB-13 does not have

¹The design wing sweep angle for cruising flight.

Table 4.4: The aircraft mathematical model parameters used in this study.

Parameter	Unit	Cherokee	ASW-19	SB-13	Gull-Wing
S	m ²	14.86	11.79	11.79	12.00
\bar{c}	m	1.6	0.822	0.797	1.02
m	kg	1089	408	435	160
I_{yy}	kg·m ²	1694	548	149.5	28.2
$C_{L\alpha}$	/rad	4.50	5.92	5.51	5.15
$C_{L\delta_e}$	/rad	0.343	0.220	0.469	0.638
$C_{M\alpha}$	/rad	-1.069	-0.633	-0.5896	-0.55
C_{Mq}	/rad	-7.83	-17.68	-5.37	-2.55
$C_{M\dot{\alpha}}$	/rad	-2.76	-3.05	0.00	0.00
$C_{M\delta_e}$	/rad	-0.63	-1.033	-0.59	-0.533
C_{D_0}		0.03125	0.0100	0.00977	0.014
C_{D_i}		0.09291	0.0196	0.01543	0.0285

the forward backward swept cranked wing like the gull wing, but only backwards sweep.

The $C_{M\delta_e}$ parameter was calculated for the gull-wing aircraft and SB-13 using a vortex lattice method.

4.7 Gull-Wing Configuration Model

The geometry of the Exulans was used to create a mathematical model. The Exulans data that were presented in Table 4.4 represents one wing sweep case. The mathematical model for the full range of wing sweep angles is presented in this section.

The variable wing sweep configuration (and therefore variable static margin) of the Exulans necessitates that static margin has to be specified at a certain sweep angle. In this document the static margin layouts are specified at 30° outboard wing sweep. 30° wing sweep was arbitrarily chosen since this is the cruise flight setting. Static margin varies with wing sweep angle for two reasons: A change in wing sweep has a significant effect on the aircraft CG and on the position of the neutral point of the aircraft.

Four different static margin layouts were investigated in this study. The four different layouts were chosen so that a large range of static margins could be evaluated with respect to handling qualities. The four layouts were 2%, 5%, 10.7% and 15% static margin at 30° wing sweep. It is important not to confuse the static margin change due to wing sweep with the different static margin layouts that are investigated.

The following observations were made with regards to the Exulans:

- The longitudinal CG of the aircraft varies with outboard wing sweep angle, since the masses of the outboard wing sections are a meaningful percentage of the all-up mass.
- The magnitude of aerodynamic damping changes significantly with a change in CG .
- Control authority is a function of longitudinal CG (and static margin) because of the short moment arm between the elevons and the CG .
- The pilot mass is a significant fraction of total aircraft mass.

The Exulans has a wing area of 12m² and a mean aerodynamic chord of 1.08m.

The methods used to calculate the parameter values used in the mathematical model set-up are explained in the following subsections. The parameter values (e.g. control authority, damping and pitch inertia) presented in this section will be referred to as ‘baseline’ values in subsequent sections.

4.7.1 Inertial Parameters

The inertial parameters relevant to the modelling of the Exulans glider are its mass, moment of inertia about the Y-Y axis and its CG .

Mass

The all-up mass of the Exulans glider comprises of the mass of the pilot, the mass of the wings and the mass of the fuselage. The pilot mass was assumed

to be 90 kg. According to Huyssen (2000) the mass of the inboard and outboard part of one wing of the Exulans glider are 13 and 9 kg respectively. The mass of each winglet on the outboard wing is 2 kg. The mass of each of the hinges of the variable sweep wings is 1 kg. The mass of the fuselage is 20 kg. The total aircraft mass (including pilot) is 160 kg.

Centre of gravity and static margin

The centre of gravity of the Exulans was calculated for different wing sweep angles. The CG 's of different components are shown in Figure 4.2. Sample mass and balance data for the Exulans layout is presented in Table 4.5.

The distance x_{cg} is measured from the leading edge of the wing on the centerline of the aircraft to the CG position. x_{cg} is positive for a CG behind the leading edge. The change in x_{cg} will be approximated as linear for the wing sweep range under investigation.

Static margin was calculated using the position of the neutral point and CG of the aircraft. The neutral point of the Exulans was calculated using a vortex lattice method. The calculation method is described in Appendix G.2.

The neutral point was calculated for different cases of wing sweep. The CG of the four static margin layouts were chosen so that the following four layouts resulted: 2%, 5%, 10.7% and 15% static margin at 30° wing sweep. The CG 's between the four layouts were altered by changing the CG 's of the fuselage and the pilot in the mass and balance calculation of the aircraft. The CG graphs for the four layouts are presented in Figure 4.3 as a function of wing sweep. The neutral point is also shown on this graph as a function of sweep. The magnitude of the static margin for a given CG layout can be visualised as the vertical distance on the graph between the neutral point line and the line of a specific CG layout. The four CG layouts of the study are referred to by their respective static margins at 30° sweep. The static margin at this sweep angle can also be visualised by means of Figure 4.3, where a bold dashed line is drawn as a measure of static margin. The line shows static margin as a percentage of mean aerodynamic chord. The graph presented in Figure 4.3 was used to calculate static margin as a function of

Table 4.5: Longitudinal mass and balance data of the Exulans (30° sweep, 10.7% @ 30° static margin layout).

Component	Mass [kg]	x_{cg} [m]	Pitch inertia around aircraft CG [kg·m ²]
Pilot	90	0.167	1.05
Fuselage	20	-0.300	6.62
Inboard wing sections	26	0.393	0.36
Wing sweep hinges	2	-0.315	0.70
Outboard wing sections	18	1.001	9.48
Winglets	4	1.855	9.98

wing sweep for the four CG layouts and the result of this is presented in Figure 4.4.

Figure 4.4 shows that the gull-wing configuration is not statically stable across the wing sweep range for two of the four different static margin layouts. These two configurations become statically unstable at the low wing sweep angles corresponding to negative static margin. In practice this means that these configurations will have a diverging nose pitch attitude if the pilot does not constantly provide correcting control inputs.

Y-Y moment of inertia

The swept gull-wing configuration has low pitch inertia when compared to other aircraft and even when compared to other tailless aircraft. Pitch inertia varies with wing sweep.

A simple approach was followed to estimate I_{yy} as a function of sweep. The aircraft was divided into different sections (Figure 4.2), as with the x_{cg} calculation, each having their own centre of gravity.

The different aircraft sections were approximated as point masses at their geometrical centroids.

The pilot was approximated as a rigid body and a point mass. This was done to simplify the inertia model. In reality, the pilot is not a rigid body or a point mass and, in the case of the Exulans, he/she is not rigidly connected

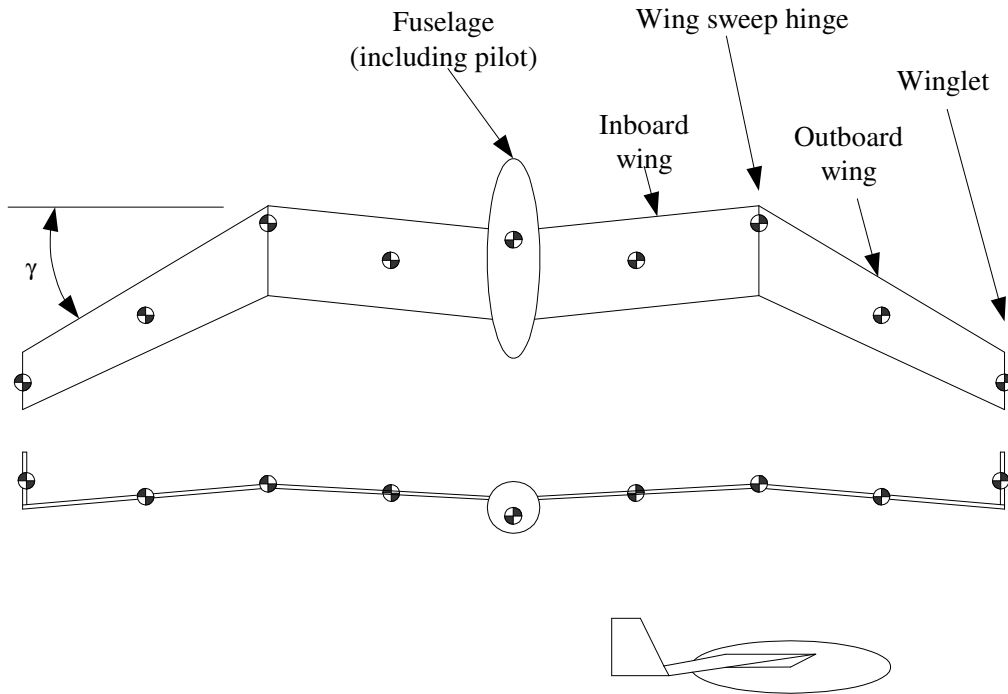


Figure 4.2: Three views of the Exulans glider showing assumed CG locations of different aircraft components. (Outboard wing sweep angle (γ) at 31°).

to the aircraft. This is because the pilot lies in the prone position in a harness mounted to the fuselage. Since the pilot is not rigidly connected to the airframe, he/she contributes less to the aircraft pitch inertia. The inertia calculation simplification can be tolerated since it is shown later (Section 5.2) that the effect on handling qualities is small if the estimation error of inertia is within 10%.

Equation 4.7 was used to evaluate I_{yy} for different wing sweep angles. The variable i in this equation represents the number of an aircraft section. The pitch inertia graphs for the four different static margin layouts are presented in Figure 4.5. An example of the pitch inertias for the different aircraft sections is presented in Table 4.5.

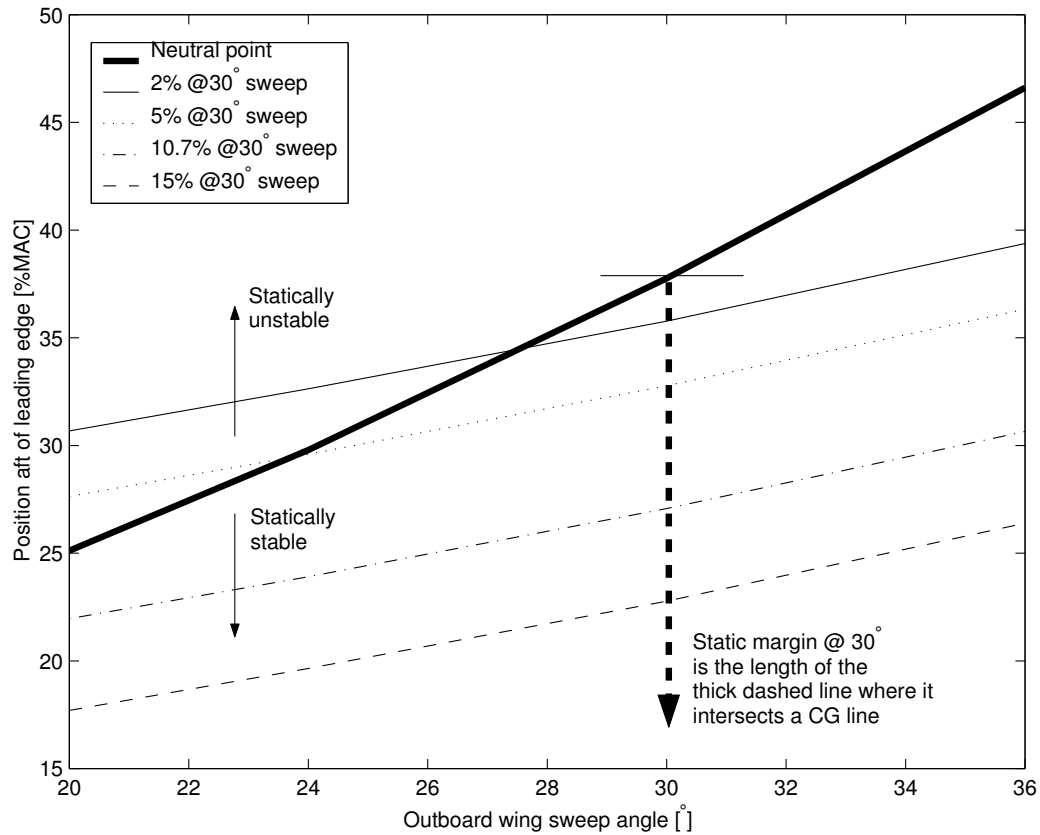


Figure 4.3: Four different CG locations and the neutral point as a function of sweep.

$$I_{yy} = \sum_{i=1}^n (x_{CG_{aircraft}} - x_{CG_i})^2 m_i \quad (4.7)$$

4.7.2 Aerodynamic Parameters

The calculation methods and results for the aerodynamic parameters are presented in this section.

Lift and pitch moment model

The lift parameters of the aircraft were obtained by consulting an aerodynamicist (Crosby, 2000) and by using a vortex lattice computer algorithm.

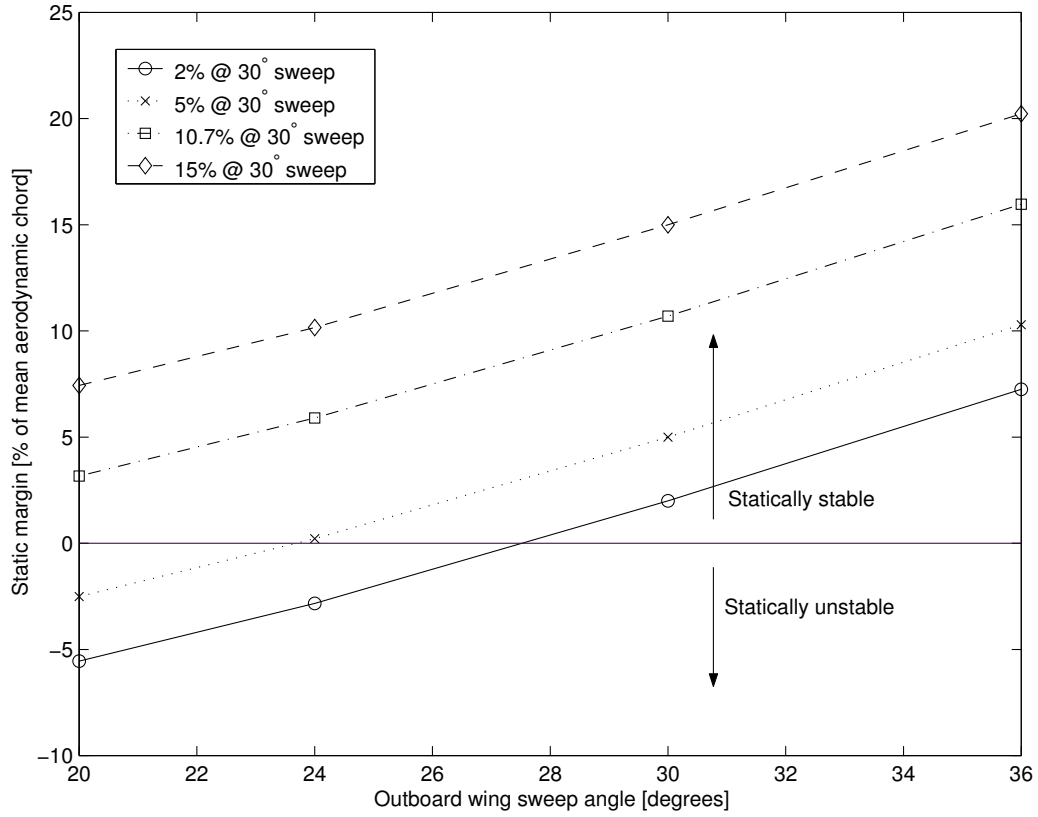


Figure 4.4: Aircraft static margin as a function of sweep angle for four different CG locations.

The total aircraft lift coefficient and the pitch moment coefficient are calculated by means of Equations 4.8 and 4.9.

$$C_L = C_{L_0} + C_{L_\alpha} \alpha + C_{L_{\delta_e}} \delta_e \quad (4.8)$$

$$C_M = C_{M_0} + C_{M_\alpha} \alpha + C_{M_{\delta_e}} \delta_e + \frac{\bar{c}}{2V_T} (C_{M_q} \dot{\theta}) \quad (4.9)$$

The aerodynamic coefficients of the Exulans were calculated for the linear aerodynamic region. The JKVLM vortex lattice method (Kay et al., 1996), was used to calculate the values of these parameters. The JKVLM code was used since it has a fast execution time and because it has a relatively simple input and output interface. JKVLM was subjected to a benchmarking

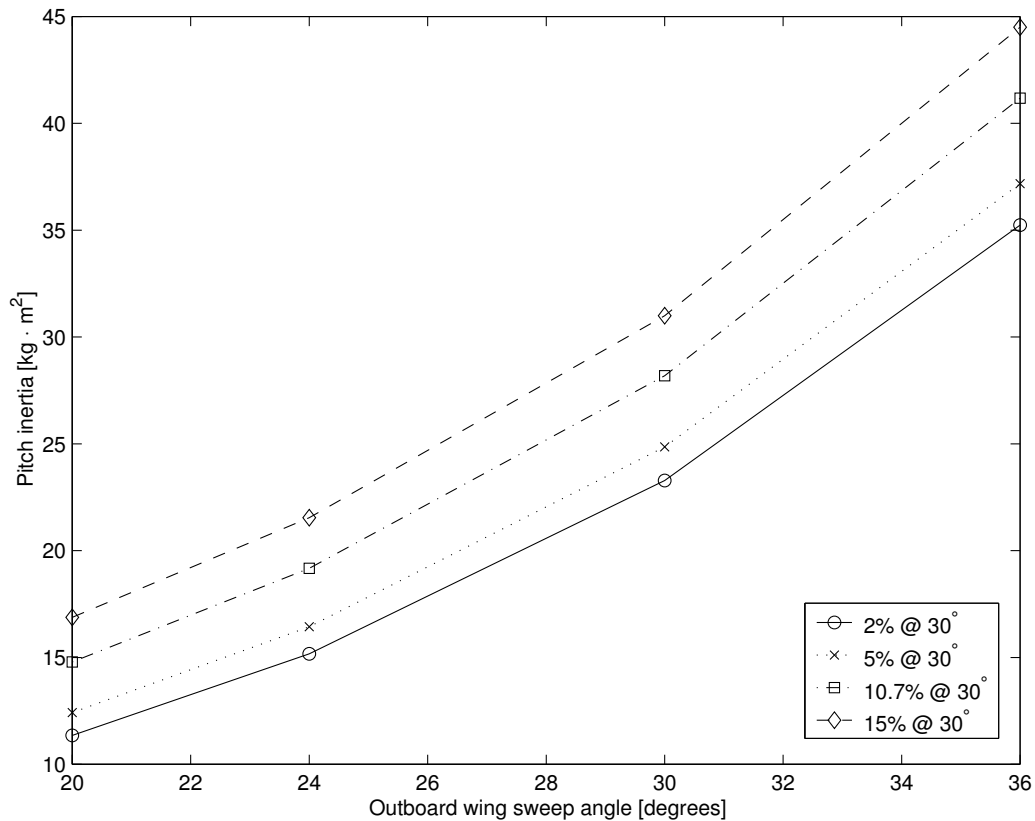


Figure 4.5: Pitch inertia (I_{yy}) as function of sweep angle for four different static margin configurations.

procedure (see Appendix G).

The following assumptions and simplifications were made in constructing the vortex lattice model of Exulans:

- The aircraft was modeled by a wing surface only. The aerodynamic effects of the fuselage were not taken into account.
- The wing was modeled as an infinitely thin plate. The effect of camber was not modeled as flat plates were used to model the wing surface. The dihedral angle of the inboard wing section and the anhedral angle of the outboard wing section were modeled.
- The outer wings were modeled as having 4 degrees of positive wing

twist (leading edge downwards). The forward sections of the flat plates are warped downwards to model wing twist.

- The effects of boundary layer flow and cross flow are not modeled with a *VLM*.
- The neutral point was calculated for an angle of attack of zero degrees.
- The outboard wing span (the lateral distance between the wing sweep hinge and the wing tip) of the Exulans *VLM* model was kept constant at 3 metres for all sweep angles that were analysed. This was done to simplify the geometry of the model. The wing chord values at the wing sweep hinge (1.1 m) and at the wing tip (0.7 m) were also kept the same for all sweep angles.

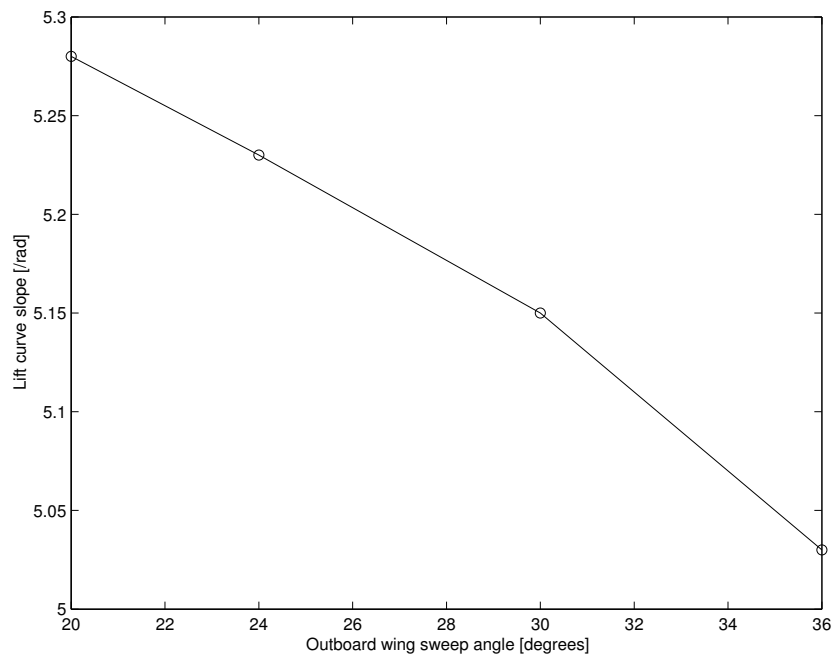
The results of the lift curve slope calculations performed with the vortex lattice method are shown in Figure 4.6.

The zero lift angle of attack was calculated incorrectly because the wing of the Exulans was modeled as an infinitely thin plate. Symmetrical sections such as the infinitely thin flat plate have a zero lift angle of attack of 0° . In reality the Exulans has a very thick wing section. This meant moment coefficients were also calculated incorrectly.

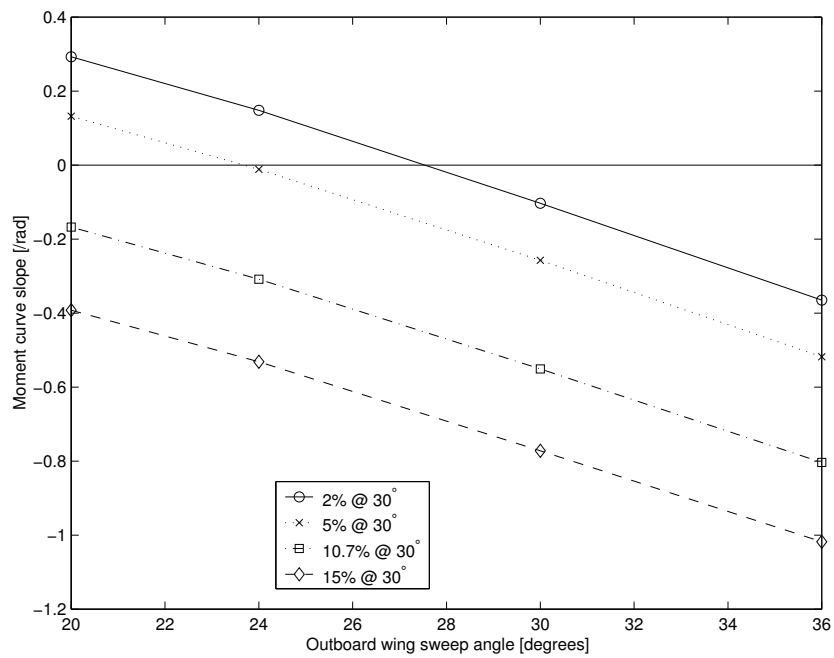
Even though the zero lift angle of attack was calculated incorrectly by JKVLM, the other stability derivative values calculated by the programme are sufficiently accurate. This was shown with the JKVLM benchmark study presented in Appendix E.

The lift curve information in Table 4.6 was obtained from Crosby (2000). This data was used to estimate the zero lift angle of attack and C_{L_0} . The information from Crosby (2000) is compared with the JKVLM values in Table 4.7.

Appendix E showed that the JKVLM C_{L_α} calculation is more accurate than that of C_{M_α} . The moment curve slope was therefore calculated by means of the relationship in Equation 4.10 using the static margin (which is specified) and the JKVLM C_{L_α} value.



(a) Lift curve slope for different outboard wing sweep angles.



(b) Moment curve slope for different outboard wing sweep angles.

Figure 4.6: $C_{L\alpha}$ and $C_{M\alpha}$ for different outboard wing sweep angles.

Table 4.6: Lift curve information from Crosby (2000)

Outboard wing sweep [degrees]	α [degrees]	C_L
24	0	0.06908
	17.8	1.7
26	6	0.625
	8	0.818
29.5	0	0.06
	2	0.244

Table 4.7: Comparison of aerodynamic data from Crosby (2000) to JKVLM results

Outboard wing sweep [degrees]	C_{L_α}	C_{L_0}	C_{L_α} JKVLM
24	5.250	0.069	5.242
26	5.529	0.046	5.215
29.5	5.271	0.060	5.159

$$\begin{aligned}
 SM &= -\frac{\partial C_M}{\partial C_L} \\
 \therefore \frac{\partial C_M}{\partial \alpha} &= -\frac{\partial C_L}{\partial \alpha} \times SM
 \end{aligned}
 \tag{4.10}$$

Table 4.7 shows that a reasonable comparison exists between JKVLM results and that of Crosby (2000). C_{L_0} varies with respect to wing sweep. The C_{L_0} value was taken as a constant value of 0.06 in order to simplify the mathematical model.

The JKVLM results for the lift curve slope (Figure 4.6) and the C_{L_0} value were used to create the lift curve for different angles of wing sweep. The JKVLM results for C_{L_α} are used instead of the aerodynamicist's information (Crosby, 2000), because it is available for a larger range of sweep angles.

In order to estimate C_{M_0} , the following procedure is followed: The physical properties of the Exulans (wing area, mass) and the estimated trim speed for a range of sweep angles are substituted into Equation 4.11. The relevant trim speeds were obtained from Crosby (2000). The air density was assumed to be $1.16 \text{ kg}\cdot\text{m}^{-3}$. A corresponding range of corresponding lift coefficients can be calculated with this information.

$$\frac{1}{2}\rho V_T^2 S C_L = mg \quad (4.11)$$

The lift coefficients can be used together with the lift equation to estimate the effective trim angle of attack. The trim angle of attack and C_{M_α} are then used to calculate a range of values for C_{M_0} . This is done by means of a moment balance around the CG of the aircraft and by noting that the moment balance equals zero for trimmed flight (see Equation 4.12).

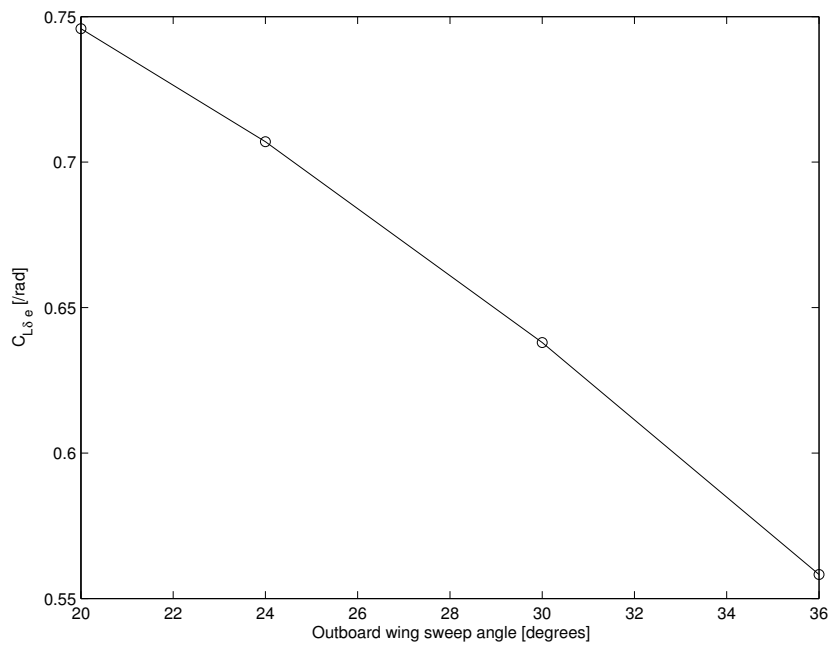
$$\begin{aligned} C_{M_0} + C_{M_\alpha} \cdot \alpha + C_{M_{\delta_e}} \delta_e &= 0 \\ C_{M_0} &= -C_{M_\alpha} \cdot \alpha - C_{M_{\delta_e}} \delta_e \end{aligned} \quad (4.12)$$

The values for $C_{M_{\delta_e}}$, $C_{L_{\delta_e}}$ and C_{M_q} were calculated using JKVLM. The elevon control surfaces on the VLM model had a chordwise dimension of 25% of the mean aerodynamic chord. The extent of the elevons were taken to be 67.5% of the semi-span to the wingtip. The results are presented Figures 4.7 and 4.8. Benchmarking of the vortex lattice method was performed for the C_{M_q} and $C_{M_{\delta_e}}$ parameters (see Appendix E and F) using wind tunnel data.

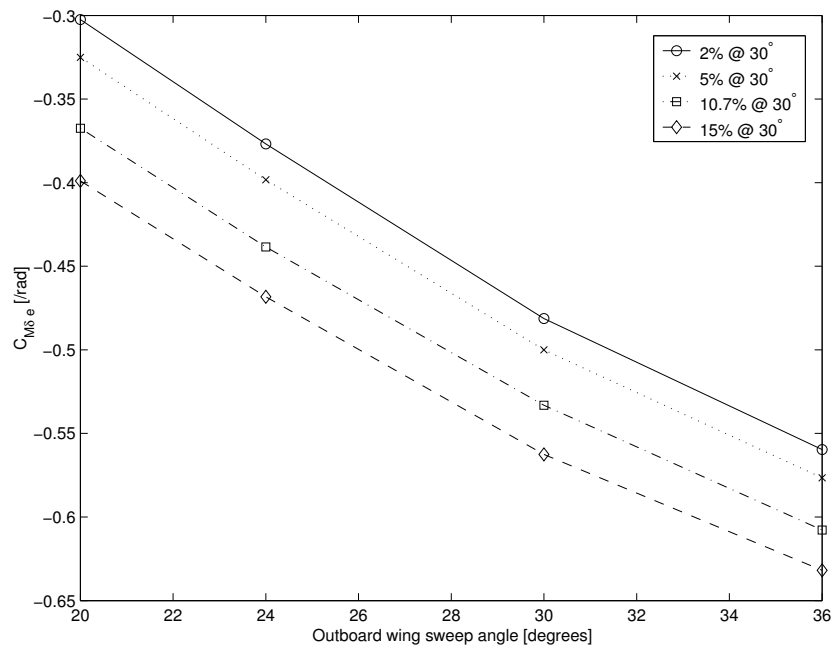
$C_{L_{\delta_e}}$ was not used in the tailed sensitivity analysis since the lift of an elevator of a tailed aircraft is small compared to the contribution of the main lifting surface. The lift produced by the elevon deflection on a tailless aircraft is significant and therefore $C_{L_{\delta_e}}$ is included in the mathematical model.

Drag Polar

The drag polar is based on the following specifications (Crosby, 2000) and the formula for a drag polar, Equation 4.13:



(a) $C_{L_{\delta_e}}$ for different outboard sweep angles.



(b) $C_{M_{\delta_e}}$ for different outboard wing sweep angles.

Figure 4.7: $C_{L_{\delta_e}}$ and $C_{M_{\delta_e}}$ for different outboard wing sweep angles.

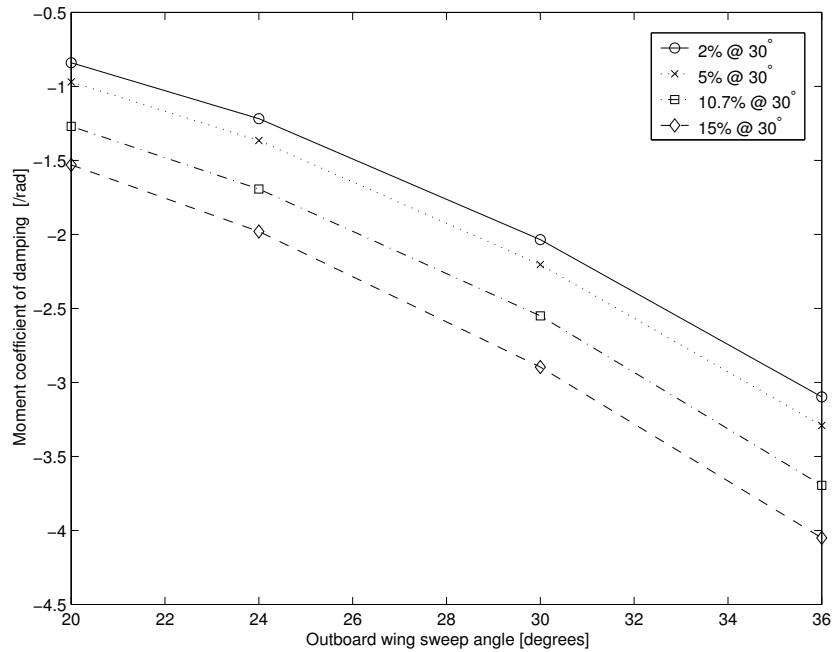


Figure 4.8: Pitch damping coefficient (C_{Mq}) for different outboard sweep angles.

- Best $\frac{L}{D}$ ratio = 25 at $C_L = 0.7$
- At the best $\frac{L}{D}$, $C_{D_0} = C_{D_i}$

$$C_D = C_{D_0} + \frac{C_L^2}{\pi A Re} \quad (4.13)$$

The values of C_{D_0} and the ARe product (clean aircraft and no flap or elevon deflection) were calculated as 0.014 and 11.1408 respectively.

4.7.3 E-point, O-Point and C-point of the Gull-Wing Configuration

Tailless aircraft offer potential advantages in terms of low drag. An elliptical lift distribution is optimal with respect to induced drag. For a tailless aircraft (without any other pitching moments acting) the maximum Oswald efficiency factor can only be achieved if the centre of gravity of the aircraft lies on the centre of pressure for an elliptical lift distribution. This point is called the ‘E-point’ according to Nickel & Wohlfahrt (1994:74).

The shape of the optimum circulation distribution for a tailless aircraft with winglets approximates the shape of a half-ellipse on the semi-span basic wing (see Figure 4.9). The centre of gravity position that coincides with the centre of lift for this lift distribution is named the O-point (ibid.: 74). The O-point is aft of the E-point in the case of a rearward swept wing, because the lift distribution corresponding with the O-point has a higher local magnitude at the wing tip than in the case of the E-point.

In addition to the E-point and the O-point, the C-Point is also defined (ibid.: 74). This is a position on the longitudinal axis that is the centre of pressure for a constant local lift coefficient along the span of the wing. This lift distribution corresponds to the maximum lift that the particular wing could possibly generate. The C-point does not correspond to an optimum lift to drag ratio. The lowest possible stall speed could be achieved if the *CG* was located in the C-point. This arrangement would be desirable for takeoff and landing, provided the handling qualities are acceptable.

In order to investigate the handling qualities of the gull-wing configuration at its optimum design point, it is required to determine whether this aircraft type has desirable handling qualities with the *CG* at the E-point (for an aircraft with a plain wing) and with the *CG* at the O-point (for an aircraft with winglets).

In the case of the Exulans, the winglets are of the all-flying type. This means that the angle of the winglets relative to the free stream may be altered by the rigging of the control run. As such the winglets can be used to produce varying magnitudes of lift. This means that the winglets can also

produce zero lift when the winglet is at the zero lift angle of attack. As a result, the aircraft could potentially be operated at either the E-point or the O-point. It is therefore required to investigate the handling qualities of the aircraft with the CG placed at the E-point and the O-point and the locations in between.

The O-point of the Exulans was calculated at various wing sweep angles. A graphical method (Figure 4.9) was used for the calculation along with the following assumptions:

- The optimum lift distribution can be approximated by the part of a half-ellipse on the basic wing planform without the winglet. This assumption is taken from Horstmann (1988).
- The wing sections of the aircraft have zero pitching moment.
- The balance of pitching moments is produced without flaps by a (hypothetical) wing torsion or wing wash-out.

The O-point calculation of the gull-wing configuration in Figure 4.9 was performed by projecting the centroid of the assumed elliptical lift distribution along the quarter chord line of the wing planform. The intersecting points of the first two sections were joined by a line. The centroid of the semi-span part of the ellipse (Section 1 + 2) was projected onto this line and projected onto the wing line of symmetry. In summary, the (ellipse) weighted average of the quarter chord line of the wing is calculated to yield the O-point. The E-point and C-point was calculated in a similar way.

The C-Point and the O-Point are close to each other in the case of the gull-wing configuration. The O-Point is behind the C-point. This is a potential handling quality problem when the flight test data of the SB-13 is taken into account. Nickel & Wohlfahrt (1994) states that the centre of gravity should be a suitable distance (at least 5% of mean aerodynamic chord) in front of the C-point in the case of a tailless aircraft in order for the aircraft to be stable. This indicates that the O-point might be inaccessible as a possible position for the centre of gravity for the gull-wing configuration. The C-point and

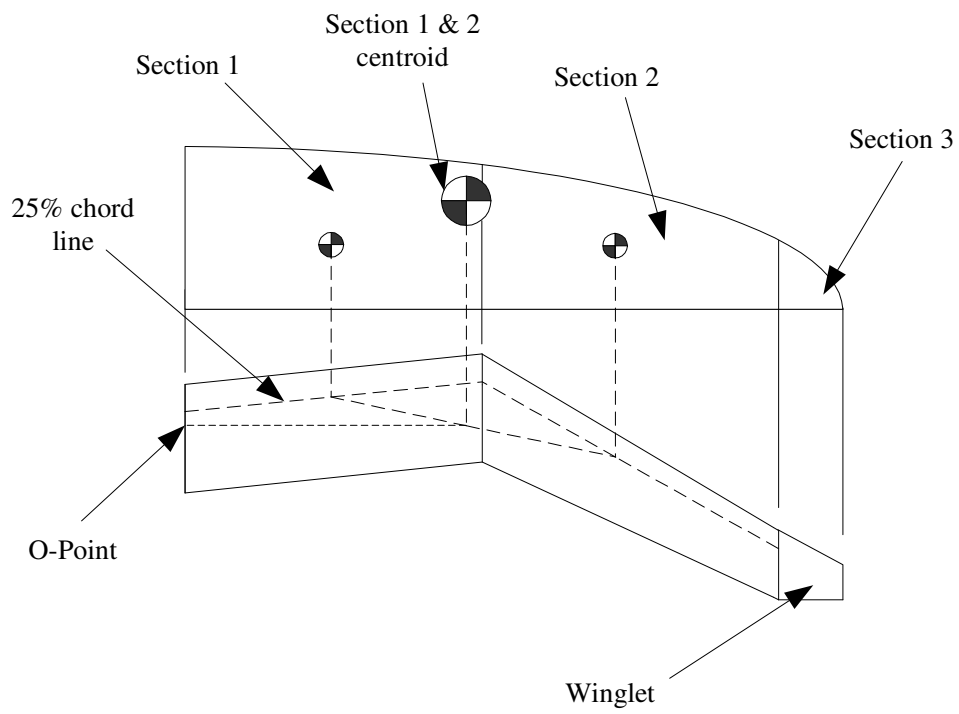


Figure 4.9: Calculation of O-Point by means of graphical method for a wing with an outboard sweep angle of 30° .

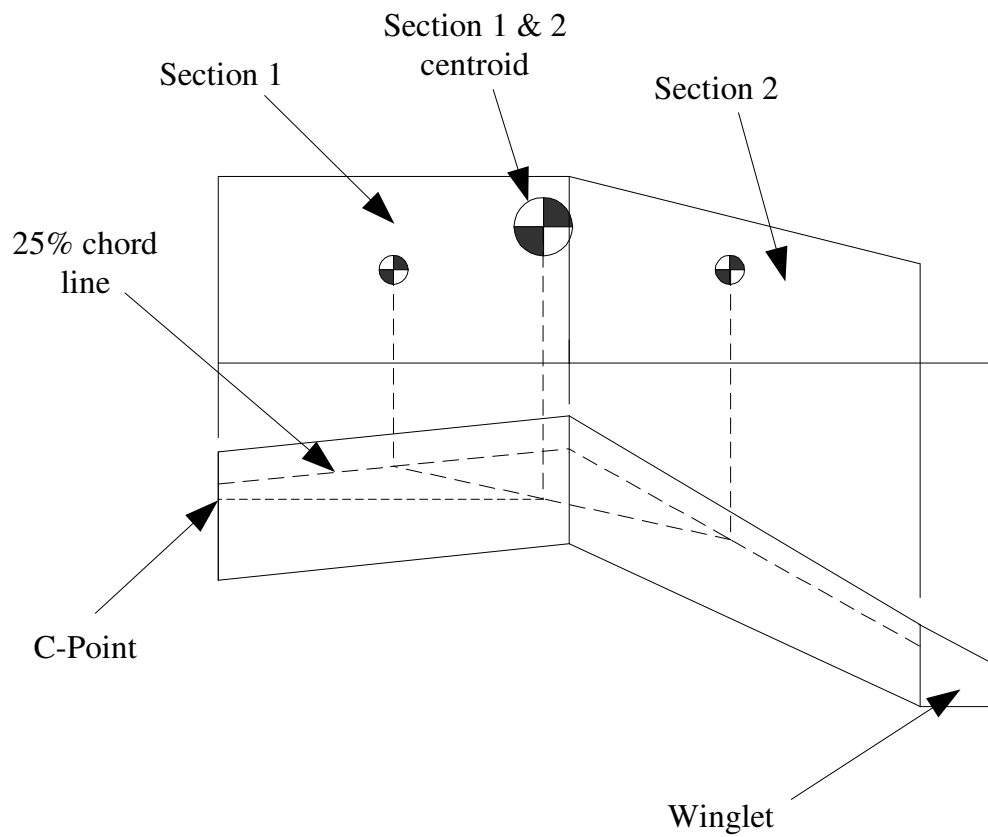


Figure 4.10: Calculation of C-Point by means of graphical method for a wing with an outboard sweep angle of 30°.

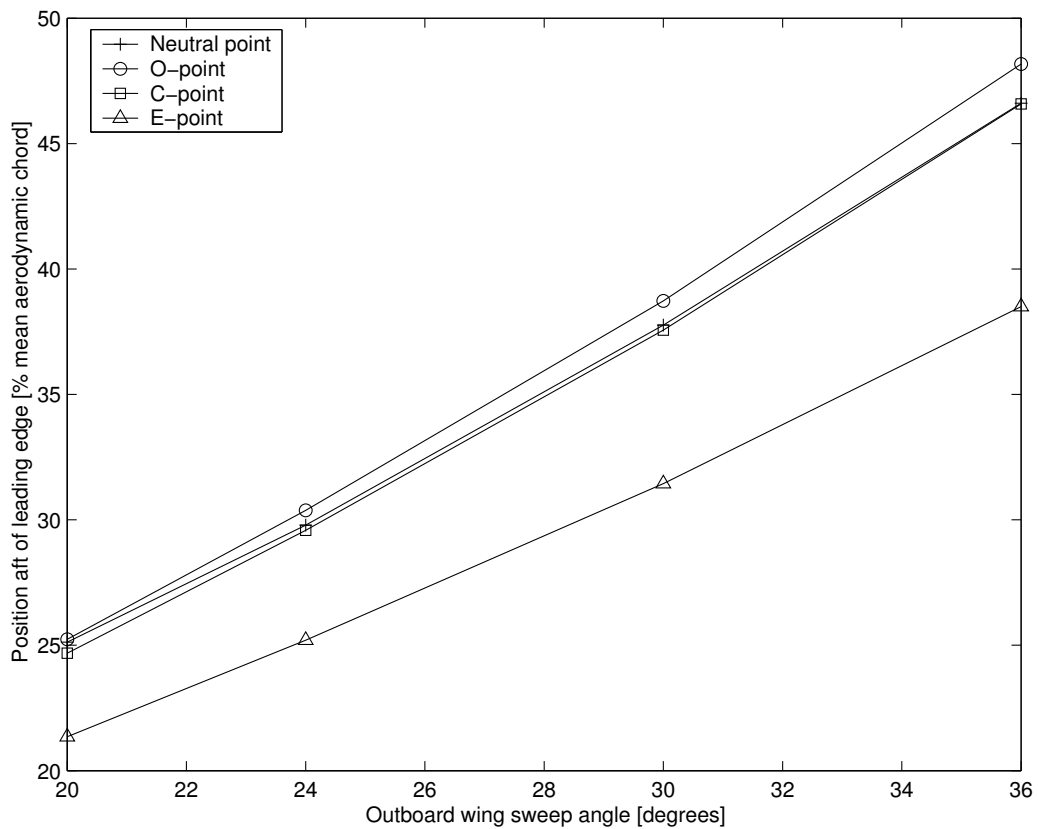


Figure 4.11: The O-point, C-point, E-point and the neutral point of the gull-wing configuration for a range of outboard wing sweep angles.

the neutral point are almost identical for the gull-wing configuration. The E-point is in front of the C-point, but it is still situated at a low static margin. It is important to verify whether good handling qualities can be expected at the CG positions close to the E-point and the O-point. It is also necessary to determine whether the maneuverability point² lies forward or aft of the O-point. If it is forward of the O-point, a pilot would not be able to control the aircraft without the assistance of stability augmentation.

The rest of the study is devoted to the investigation of whether or not the Exulans aircraft, as an example of a gull-wing configuration, has satisfactory handling characteristics with its CG positioned at various magnitudes of static margin. Special consideration will be given to static margins that have CG positions that are coincident with either the E-point or the O-point.

4.8 Disturbance models

The disturbance models used for simulation of wind gusts and elevon inputs are described here. These disturbance models were used for the gull-wing configuration sensitivity study chapter and simulation results presented in subsequent chapters.

4.8.1 Gust Disturbance

A vertical wind gust is modeled by using the equations of the angle of attack and the pitch rate. The disturbance is introduced as described in Equation 4.1. This gust model is presented by Etkin (1972) and simulation results using this gust model are presented by Mönlich & Dalldorff (1993). The gust model uses the assumption that the effect of a vertical gust on an aircraft flying through the gust is equivalent to a pitch rate disturbance. A graphical representation of the pitch rate disturbance is presented in Figure 4.12.

The implementation of the gust disturbance is presented in Equation 4.14.

²The maneuverability point is a CG position where the aircraft has low or negative static margin, but where the pilot is still able to fly the aircraft without excessive pilot workload.

$$q_{rel} = q + q_g \quad (4.14)$$

$$= q + \dot{w}_g/V_e \quad (4.15)$$

The variations in trim airspeed are assumed to be small according to small disturbance theory and are therefore held constant. The vertical gust velocity (w_g) and its derivative with respect to time are presented in Equation 4.16

$$\begin{aligned} w_g &= W_g \left(\frac{1}{2} \right) (1 - \cos(\omega t)) \\ w_g &= W_g \left(\frac{1}{2} \right) \left(1 - \cos \left(2\pi \left(\frac{V_e}{\lambda} \right) t \right) \right) \\ \dot{w}_g &= \left(\frac{W_g \pi V_e}{\lambda} \right) \sin \left(2\pi \left(\frac{V_e}{\lambda} \right) t \right) \end{aligned} \quad (4.16)$$

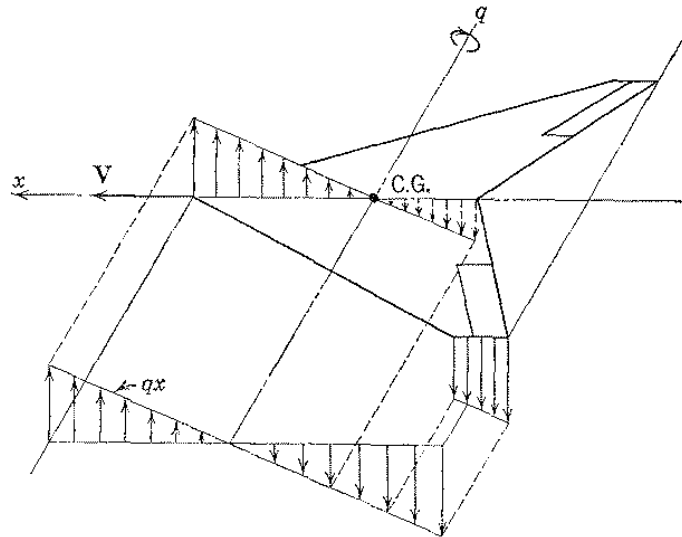


Figure 4.12: Wing velocity distribution due to pitching. (Etkin, 1972:270)

Equation 4.14 is valid for long wavelengths only. The wavelength of the vertical gust inputs for all the simulations was taken as 50m and $W_g = 2$ m/s.

The vertical gust was introduced after 1 second of simulation time for all the simulations that were performed on the different aircraft models.

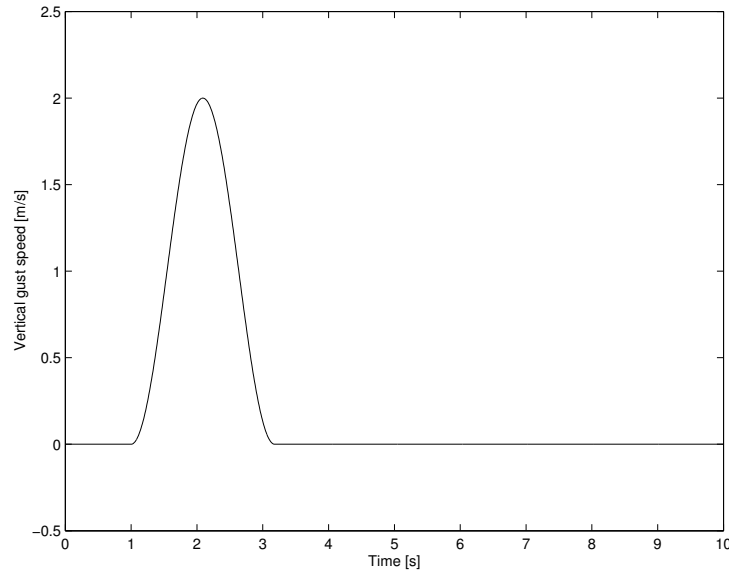


Figure 4.13: The 1 – cos vertical gust disturbance. (Mönnich & Dalldorff, 1993)

4.8.2 Elevon Step Input

A step input was used for the pitch control response simulations that were performed in this study. The input was introduced after 1 second for all simulations. The step input that was used had a magnitude of negative 1 degree elevon deflection (δ_e). The sign convention followed throughout the study means that the negative elevon deflection (elevon up) causes an aircraft nose up rotation.

The boundary layer around the elevon is not modeled in the simulation and as a result no control stick dead band is simulated. The simulation results show that the aircraft responds immediately to the control input because of this. This was done to investigate the effect of control input in isolation with regards to the effects of other dynamics.

Chapter 5

Gull-Wing Sensitivity Analysis

The results and conclusions of the gull-wing configuration handling quality study are dependent on the values of the input parameters of the aircraft model. The exact magnitudes of these parameters have not been measured, but were estimated by calculation. In order to have sufficient confidence in the conclusions of this study, it was required to gauge the effect of estimation errors on the predicted pitch response (and hence, handling qualities) of the aircraft. The sensitivity study was used to assess the confidence level of the predicted aircraft pitch responses and as a result, the conclusions presented in this study.

The static margin, damping coefficient, pitch inertia and control authority were identified in Section 4.5.3 as the most influential variables with respect to pitch dynamics. The *CG* can be varied (within practical limits) on an actual aircraft to achieve a certain static margin. The static margin can then be verified by measurements, but the remaining variables cannot be altered as easily. The accuracy with which these parameter values are predicted is therefore important. As a result, the sensitivity study was focussed on the parameters other than static margin.

5.1 Baseline and method

The Exulans mathematical model was used for the analysis. The sensitivity study was performed on an Exulans with 30° outboard wing sweep angle and a static margin of 10.7% at 30° wing sweep. This applies to all simulation results presented in this chapter. The study comprises of time domain simulations with a gust disturbance after 1 second. The gust disturbance is as documented in Section 4.8. The parameter values of the Exulans mathematical model were varied over the following ranges for the purpose of the sensitivity study:

- The pitch inertia was varied from -10% to +10% with respect to the baseline. This narrow range was chosen for pitch inertia since it can be determined within reasonable accuracy prior to the construction of an aircraft. It can also be fine tuned (within practical limits) once an aircraft is built.
- The pitch damping coefficient was varied from -50% to +50% with respect to the baseline. This range was chosen with the guidance of the C_{M_q} benchmark study (Appendix E). The benchmark work indicated that pitch damping estimated with a *VLM* differs by as much as 50% from the actual value.
- The elevon control authority was varied from -20% to +20% with respect to the baseline. This range was chosen with the guidance of the $C_{M_{\delta_e}}$ benchmark study (Appendix F). The benchmark work indicated that the pitch control authority estimated with a *VLM* differs by as much as 20% from the actual value.

The baseline parameter values of the sensitivity analysis are presented in Table 4.4 under the gull-wing column. The parameter values were varied individually during each simulation, while all the other parameters were kept at the baseline values. All time domain simulations were performed with a true airspeed speed of 82.4 km/h, which is the design trim speed at 30° outboard wing sweep according to Crosby (2000). The simulations of the

sensitivity study were performed with a time step of 0.01 seconds (i.e., samples at 100 Hz). The justification for this choice of time step size is presented in Appendix D.

The modal parameters (natural circular frequency and damping) were also calculated for the baseline model and the different models of the sensitivity study. The sensitivity with respect to a certain parameter was evaluated by visual inspection of the time domain simulation results and the change in the modal parameter values from the baseline. The baseline values for the sensitivity study and the modal parameters are presented in Table 5.1.

Table 5.1: Baseline parameter values used for the sensitivity study (30° sweep gull-wing configuration with a 10.7% static margin at 30° sweep).

Parameter	Unit	Baseline value
I_{yy}	kg·m ²	28.2
C_{M_q}	/rad	-2.55
$C_{M_{\delta_e}}$	/rad	-0.533
$\omega_{n_{sp}}$	rad/s	10.28
ζ_{sp}		0.592
ω_{n_p}	rad/s	0.49
ζ_p		0.075

The modal characteristics were estimated using numerical techniques (theory presented in Appendix B), as opposed to the analytical approximations of Section 4.5. The numerical techniques are more accurate since fewer assumptions are made in the estimation than in the case of the analytical answer. The numerical technique uses a linearised model associated with some trim condition to calculate the modal characteristics. A comparison between the two methods is presented in Table 5.2. The phugoid mode frequency approximation does not show good agreement with that of the numerical method. The phugoid damping approximation was not calculated because the approximation is known to be inaccurate. The short period mode approximation shows better correlation with the numerical method. These results are in agreement with the discussion on the accuracy of the approximations as presented in Stevens & Lewis (1992:210).

Table 5.2: Comparison of modal characteristics estimated by numerical methods and analytical approximations (30° sweep gull-wing configuration with a 10.7% static margin at 30° sweep).

Parameter	Unit	Numerical	Analytical
$\omega_{n_{sp}}$	rad/s	10.28	8.44
ζ_{sp}		0.59	0.44
ω_{n_p}	rad/s	0.49	0.10

5.2 Pitch Axis Inertia

The results of the pitch inertia sensitivity study simulations are presented in Figures 5.1 to 5.4.

The pitch inertia of the Exulans is low compared to its roll and yaw inertia. The pitch inertia was varied from 10% below to 10% above the baseline value of 28.2 kg·m² (the 30° sweep value at 10.7% static margin). The inertia changes had a small effect on pitch rate and attitude. The phugoid mode is almost unaffected by a change in inertia, but the short period mode is affected by the change. This can be seen from the change in the small ‘hump’ (left side of the graph in Figure 5.4) of the attitude response. The inertia changes had a noticeable effect on angle of attack dynamics.

The sensitivity of pitch inertia with respect to the natural frequency and damping ratios of the aircraft modes is shown in Tables 5.3 and 5.4. The 10% change in pitch inertia has no effect on phugoid natural frequency and a small effect on phugoid and short period damping ratio. It causes a 5% change in short period natural frequency. The effect of this on handling qualities can be assessed by using the thumbprint criterion (see Section 3.3). If one bears in mind that the lines on the thumbprint graph do not represent absolute borders, but rather smooth transitions, it can be argued that a 0.6 rad/s (or 5% from the baseline) change in short period natural frequency does not represent a drastic change in handling qualities. Such a difference would not have the effect of changing the pilot opinion rating from ‘Satisfactory’ to ‘Poor’. The estimation error of inertia can be contained within 10% and therefore the baseline value of inertia can be used for all handling qualities

analyses in this study.

Table 5.3: Sensitivity of circular natural frequency with respect to pitch inertia.

Inertia [% change]	ω_{n_p}	[% change]	$\omega_{n_{sp}}$	[% change]
-10	0.493	No change	10.842	5.44
Baseline	0.493		10.283	
10	0.493	No change	9.808	-4.62
Average sensitivity [%/%]		None		-0.50

Table 5.4: Sensitivity of damping ratio with respect to pitch inertia.

Inertia [% change]	ζ_p	[% change]	ζ_{sp}	[% change]
-10	0.076	1.60	0.598	1.06
Baseline	0.075		0.592	
10	0.074	-1.47	0.587	-0.79
Average sensitivity [%/%]		-0.15		-0.09

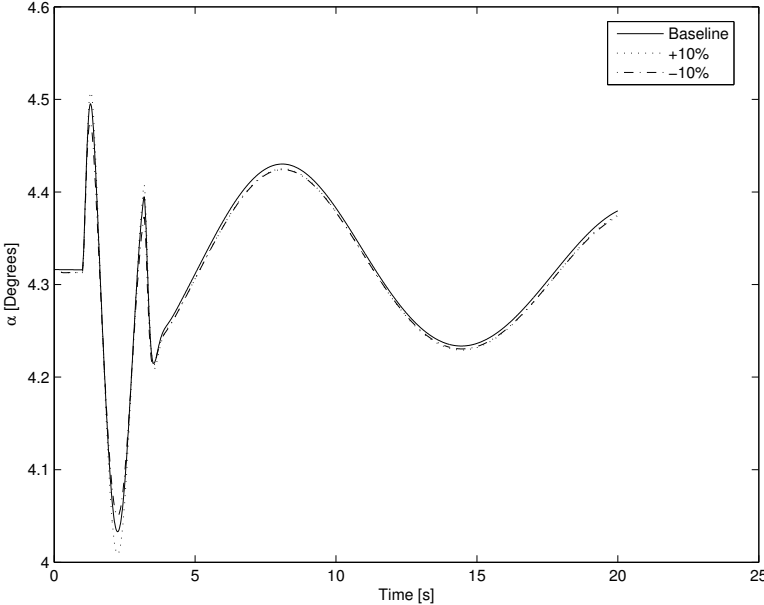


Figure 5.1: Gust response of aircraft angle of attack (α) at different pitch axis inertias.

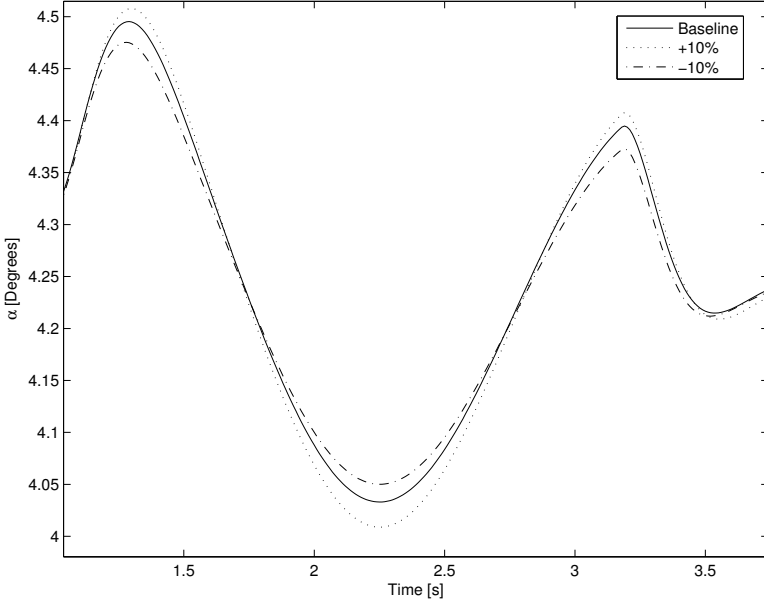


Figure 5.2: Magnified gust response of aircraft angle of attack (α) at different pitch axis inertias.

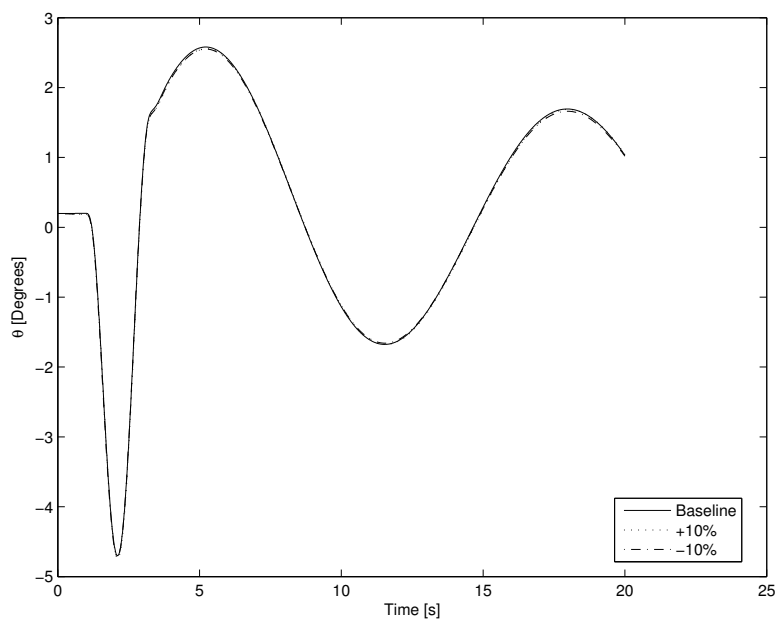


Figure 5.3: Gust response of aircraft attitude (θ) at different pitch axis inertias.

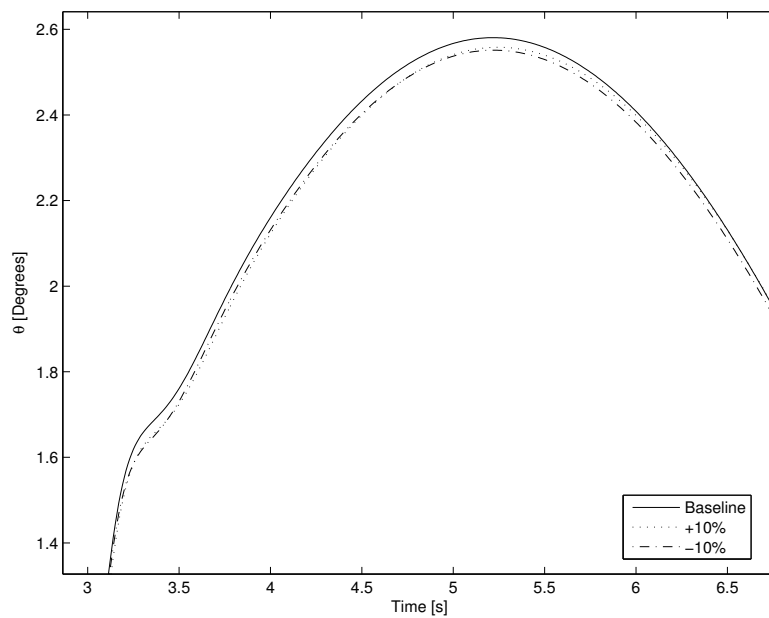


Figure 5.4: Short period gust response of aircraft attitude (θ) at different pitch axis inertias.

5.3 Pitch Damping Coefficient

The pitch damping coefficient changes significantly with respect to CG in the case of a tailless aircraft. In the case of a tailed aircraft the distance from the tail to the centre of gravity and the lift curve slope of the tailplane are the most important parameters in the calculation of the aerodynamic damping coefficient of the aircraft. Changes in centre of gravity are usually small as a percentage of the distance to the tail and hence the change in damping coefficient due to a centre of gravity change is also small. This is not the case for a tailless aircraft, since its damping ratio is a function of the planform of the main lifting surface. A change in the CG position therefore has a significant effect on the damping coefficient of a tailless aircraft.

Simulations with the gull-wing model were performed where the static margin was held constant at the baseline configuration of 10.7%. The pitch inertia was also held constant. The pitch damping coefficient was varied by 50% above and below the baseline. The results of these simulations are presented in Figures 5.5 and 5.6. The natural frequency and damping ratio of the aircraft modes were calculated for the different aerodynamic damping cases. These results are presented in Table 5.5 and 5.6.

The results of the sensitivity study show that a 50% change in the aerodynamic damping coefficient causes a larger than 7% change in phugoid and short period frequency. The change in damping has a significant effect on damping ratio for both the short period (larger than 19% change) and the phugoid (larger than 14% change) damping ratio. When the thumbprint graph (Figure 3.1) is examined, it can be seen that such a change in short period damping ratio can have a significant effect on pilot opinion. The inaccuracy in the calculation of the value of the damping ratio is not so severe that it will invalidate the conclusions produced by the handling quality study. A 50% change in damping ratio will not change the pilot opinion result to the extent that the analysis is invalid. Appendix E showed that a 50% inaccuracy is a worst case scenario for C_{M_q} . It is more likely for the case of the Exulans (with forward and backward wing sweep) that the inaccuracy will be 20%. It can therefore be concluded that the uncertainty in the aerodynamic

damping ratio is large enough for it to be a variable in the handling quality investigation, but that C_{M_q} should be varied by 20% above and below the baseline.

Table 5.5: Sensitivity of natural frequency with respect to pitch damping coefficient.

Damping [% change]	ω_{n_p} [% change]	$\omega_{n_{sp}}$ [% change]
-50	0.540	9.68
Baseline	0.493	10.283
50	0.456	-7.55
Average sensitivity [%/%]		-0.17

Table 5.6: Sensitivity of damping ratio with respect to pitch damping coefficient.

Damping [% change]	ζ_p [% change]	ζ_{sp} [% change]
-50	0.064	-14.17
Baseline	0.075	0.592
50	0.086	14.30
Average sensitivity [%/%]		0.28

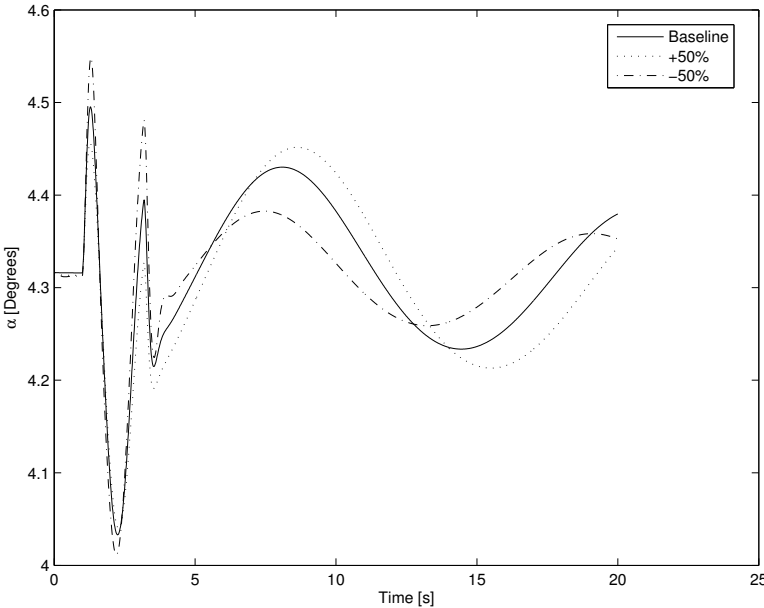


Figure 5.5: Gust response of aircraft angle of attack (α) at different damping coefficient values.

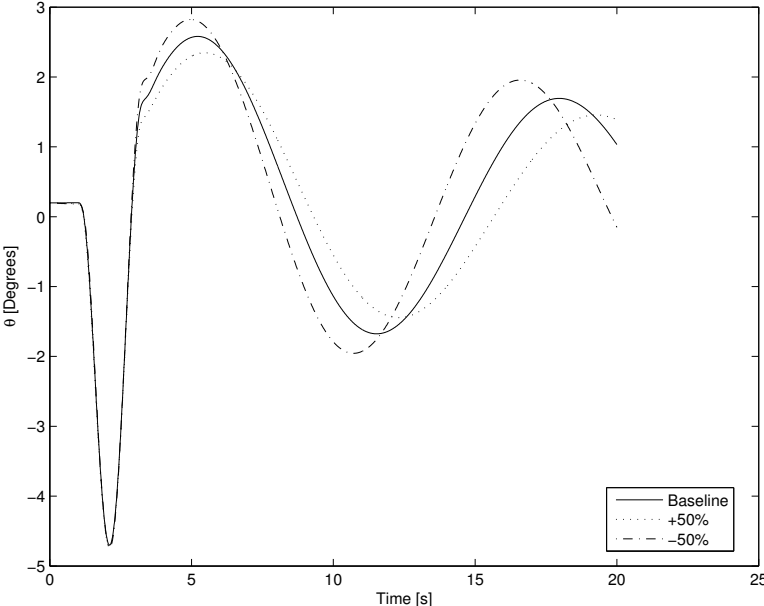


Figure 5.6: Gust response of aircraft attitude (θ) at different damping coefficient values.

5.4 Elevon Control Authority

The sensitivity of the aircraft pitch attitude response to varying degrees of control authority was investigated with time domain simulations. This was done to assess the impact of the estimation error of the $C_{M_{\delta_e}}$ parameter on handling qualities. $C_{L_{\delta_e}}$ is predicted with sufficient accuracy (see Appendix F) and therefore the sensitivity of the aircraft response with respect to this parameter was not investigated.

Control authority (the magnitude of $C_{M_{\delta_e}}$) of the elevons influences the magnitude of the response to an elevon control input. Control authority must not be confused with the gearing to the elevon, since it is a function of the control surface aerodynamics. The control authority can be modelled as a gain in the aircraft attitude control loop.

Three cases of control authority were investigated in the sensitivity analysis. The baseline control authority as presented in Table 4.4 for an aircraft with an outboard wing sweep of 30° was used in one simulation. Pitch inertia, static margin and aerodynamic damping were kept constant in simulations while control authority was varied. For one simulation the control authority was 20% higher than the baseline and for the other the control authority was 20% lower than the baseline. This variance in the control authority corresponds to the estimation error of the parameter (Appendix F). The lift due to elevon deflection or $C_{L_{\delta_e}}$ was kept at the baseline value for all simulations.

The simulations were performed with a -1° elevon step input at 1 second after the start of the simulation. The simulation results are presented in Figures 5.7 to 5.8.

The simulation results show that the natural frequencies and damping ratios of the aircraft's dynamic modes are unchanged by different control authorities. Control authority has a significant influence on the magnitude of the pitch attitude of the aircraft following a control input. The effect on the magnitude is shown in Table 5.7. These results show that the magnitude changes by 1% (on average) from the baseline for every 1% change in the control authority. This is a significant change and therefore the estimation

error for this parameter will have a definite effect on handling qualities. The $C_{M_{\delta_e}}$ parameter therefore has to be varied by 20% from the baseline for handling quality studies involving control authority.

Table 5.7: Sensitivity of pitch attitude (θ) amplitude with respect to $C_{M_{\delta_e}}$.

$C_{M_{\delta_e}}$ [% change]	Maximum θ amplitude [°]	[% change]
-20	4.910	-21.54
Baseline	6.258	
20	7.645	22.16
Average sensitivity [%/%]		1.09

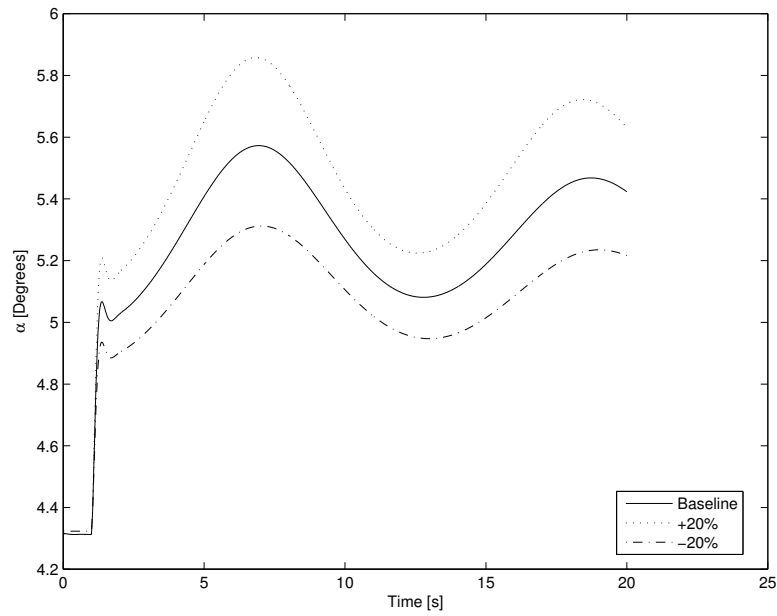


Figure 5.7: Control input step response of aircraft angle of attack (α) at different control authority aircraft configurations.

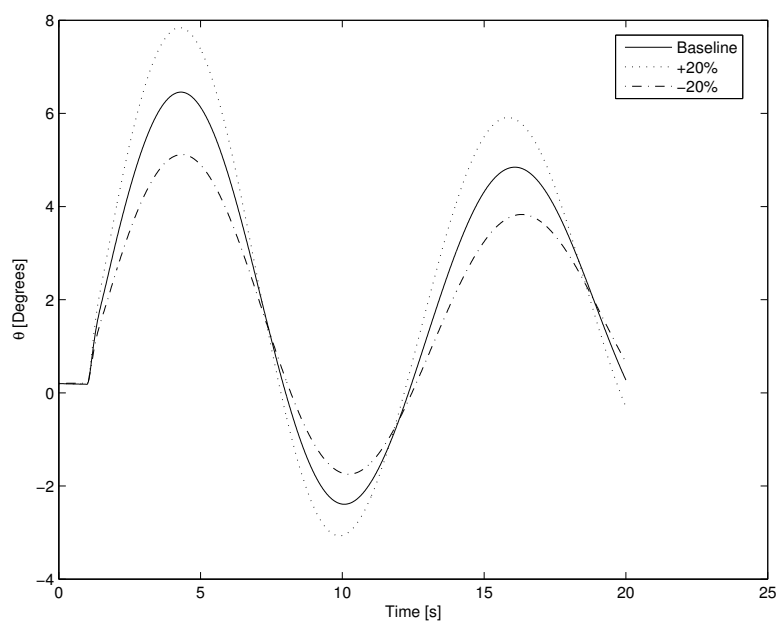


Figure 5.8: Control input step response of aircraft attitude (θ) at different control authority aircraft configurations.

5.5 Conclusion of Sensitivity Analysis

The estimation error of pitch inertia (for an aircraft the size of the Exulans) is not significant enough to have a noticeable effect on the outcome of a handling quality analysis of the gull-wing configuration. The inertia will therefore not be a variable in the handling quality analyses presented here.

Aerodynamic pitch damping has a significant influence on the aircraft attitude, natural frequency and damping ratio of the aircraft modes. The C_{M_q} parameter value will be varied by 20% in the handling quality study because this is the estimation error of this parameter. The effects of this error on handling qualities need to be assessed.

Elevon control authority has a significant influence on aircraft attitude following a control input. The estimation error of this parameter is 20% above and below the baseline value. The handling quality study will therefore include this variance to investigate the effects of this estimation error.

The effects of only static margin, aerodynamic pitch damping and elevon control authority were investigated in the handling quality analyses documented in subsequent chapters. The influence of pitch inertia is not investigated further. This is because it does not have a sufficiently significant effect on the dynamic modes and because it can be estimated with reasonable accuracy.

Chapter 6

Time Domain Analysis

Time domain handling quality analyses of the Exulans are presented in this chapter. The handling characteristics of the gull-wing configuration (using the Exulans as representative example) were investigated by means of step elevon control input simulations and gust response simulations. The C-star handling quality criterion was applied to the simulation results. The Exulans gust responses were also compared to those of an existing tailed glider (ASW-19), an existing tailless glider (SB-13 Arcus) and a powered aircraft (Piper Cherokee) in gliding (engine off) flight.

6.1 C-star Criterion Analysis

The C-star analysis method is explained in Section 3.5. This type of analysis was applied to different combinations of sweep and static margin of the Exulans. The different cases of the gull-wing configuration that were analysed are defined in Appendix I.1.

The results of one set of C-star analyses are presented here (Figure 6.1) and the rest are presented in Appendix I.5. Figure 6.1 is presented as an arbitrary sample of a C-star analysis result.

The following conclusions can be made from the C-star analysis:

A response is favourable with respect to the C-star criterion when it falls inside the C-star boundaries and when it does not exhibit a lightly

damped oscillation. The C-star response of most of Exulans cases that were investigated fall outside the favourable C-star boundaries. This is especially evident during the first 0.6 seconds of the normalised response. After the initial 0.6 seconds most of the responses fall within the C-star boundaries. Almost none of the cases exhibited a lightly damped oscillation, as the steady state C-star response converges quickly. It may therefore be concluded that the initial response of the Exulans to a step response is unfavourable. The handling qualities improve after the initial response according to this method.

Static margin and outboard wing sweep have the largest influence on handling qualities according to the C-star analysis. This is evident from Figures I.51 and I.52: The 24° sweep cases almost fall within the ‘powered landing’ (thick dashed line) C-star boundaries, while the 30° cases have a very high initial overshoot outside the C-star boundaries. The lower sweep cases seem to have more favourable handling qualities according to this observation.

The estimation error of control authority has a significant effect on C-star handling qualities at low sweep angles (24°). Higher moment control authority has the consequence of a large initial overshoot as can be seen in Figure 6.1. This figure shows that the low control authority case falls completely within the ‘powered landing’ boundaries, while the high and baseline cases have an initial overshoot. Figure I.54 shows that the effect of the estimation error is of lesser importance at 30° sweep since all the cases fall outside the acceptable boundaries. The general trend is that less moment control authority leads to a more favourable C-star handling quality evaluation.

Figure I.55 shows the effect on the estimation error of the aerodynamic damping coefficient on the handling qualities as predicted by the C-star method. This results indicate that damping does have an influence on handling qualities, but that it is not significant.

The C-star response has an important conclusion with regards to the CG position of the pilot relative to that of the aircraft CG . The third term of Equation 3.3 tends to translate the C-star response to the right. This means that pitch acceleration and the distance l have a significant effect on the handling qualities. l is the distance from the aircraft CG to the acceleration

sensory organ of the pilot (the ear). It is advisable for the aircraft designer to minimise this distance, because if the pilot is far from the CG he or she will experience unpleasant pitch accelerations, leading to poor handling qualities. In the case of the gull-wing configuration this is best achieved by placing the pilot on the aircraft CG if other design considerations permit this. The distance l is zero with an upright sitting pilot coincident with the aircraft CG . l is equal to the distance from the pilot hip to the head for a pilot in the prone position (with the hip coincident with the aircraft CG).

The C-star analysis method has some limitations, which have an influence on the value of the conclusions made from it:

- Statically unstable and marginally stable cases of sweep and static margin (eg. configurations 45 and 54) can not be evaluated using the C-star method. The reason for this is that stick fixed simulations results are used to calculate the C-star response. The stick fixed simulations are divergent for marginally stable and unstable cases and therefore the C-star criterion cannot be applied.
- The effect of a pilot can not be evaluated with the C-star method as in the case of the Neal-Smith method (see Section 7.4).
- The C-star criterion is more difficult to interpret than other handling qualities criteria. If a response falls outside the boundary, it does not give a good indication of how the response could be improved. This is one of the deficiencies of the method as described in Neal & Smith (1970).

These limitations make it necessary to evaluate the conclusions of the C-star method together with other handling quality analysis methods. This will be done in Section 7.5 where the C-star results will be compared with frequency domain analysis results. Without comparison to other methods, the general conclusion of the C-star method is that the Exulans will have marginally acceptable handling qualities during landing (associated with low sweep angles) and unacceptable handling qualities during rapid manoeuvring.

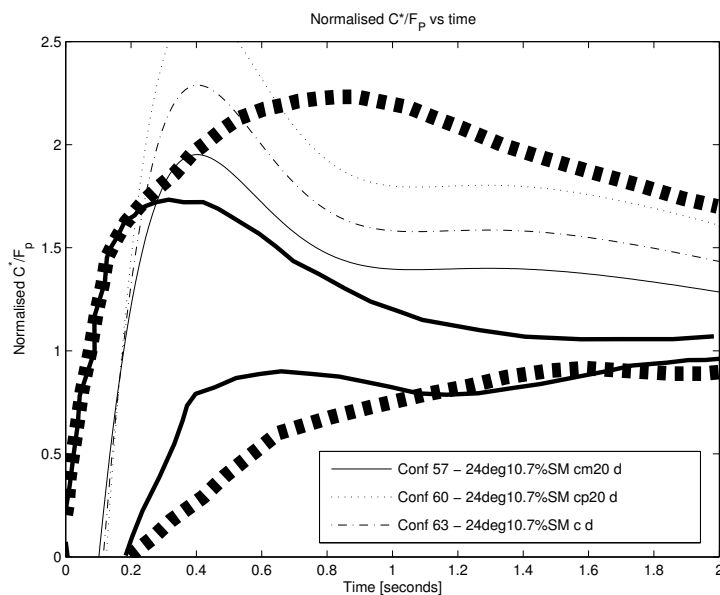


Figure 6.1: The C-star analysis for all control authority variations at 24° sweep with the baseline aerodynamic damping at a 10.7% (at 30°) static margin configuration. (Configurations 57, 60, 63)

6.2 Comparative Simulations

The gust response of the Exulans was compared with a similar class tailless aircraft and a similar class tailed aircraft. As a matter of interest, the Exulans response was also compared to the response of a powered aircraft in gliding flight. The Piper Cherokee was chosen as a representative powered aircraft.

The SB-13 was chosen as a representative tailless aircraft. This aircraft is a standard class glider and was developed in the 80's and 90's.

The ASW-19 was chosen as a representative conventional aircraft with which the Exulans can be compared. This aircraft is known to have very good handling characteristics as well as being a high performance glider.

'Stick-fixed' simulations were used to compare the different aircraft types. The time responses of the different aircraft were plotted on the same axes and evaluated.

A similar study has been performed which involved the SB-13 and the ASW-19 (Mönnich & Dalldorff, 1993). This study found that the gust

responses were important in determining the relative handling qualities of the two aircraft. A $1 - \cos$ gust disturbance was used in all simulations. The gust model is discussed in Section 4.8.1.

Three Exulans layouts were used as part of the comparative study. A low outboard wing sweep configuration (24° , static margin of 15% at 30°) and a high wing sweep configuration (36° , static margin of 5% at 30°) were used. A medium sweep (30° , static margin of 2% at 30°) case was also included in the analysis. The low and high sweep Exulans models have a static margin of 10% at the particular sweep angle. The SB-13 and the ASW-19 models used in the simulations also have static margins of 10%. The Exulans has lower trim design speeds than the other aircraft used in the comparative study. This makes a direct comparison between all the aircraft difficult and limits the analysis to a qualitative evaluation of the time responses. Both the ASW-19 and the SB-13 were trimmed at 120km/h for the simulations. The Exulans models were trimmed at 55.3, 82 and 109.4km/h for the 24° , 30° and 36° sweep cases respectively.

The results of the comparative study are presented in Figures 6.2 to 6.8. These figures show the attitude response to a $1 - \cos$ wind gust disturbance. The short period attitude responses of Figure 6.3 were translated vertically (to change the reference attitude to zero degrees) and superimposed for comparison purposes. The result is presented in Figure 6.4. The same superposition and translation was done with the results of Figure 6.6 and the results are presented in Figure 6.7.

The following observations can be made from the results presented in this section:

- The SB-13 has a weakly damped short period oscillation. The short period oscillation is the ‘bump’ between 1.5 and 2 seconds after the start of the simulation. This may contribute to poor handling characteristics.
- The ASW-19 and Cherokee have strongly damped short period modes, to the point that it is not visible on the attitude response of the aircraft.
- The Exulans has a visible short period response (the ‘bump’) for the low (24°) and high (36°) sweep cases. Both these cases have a 10%

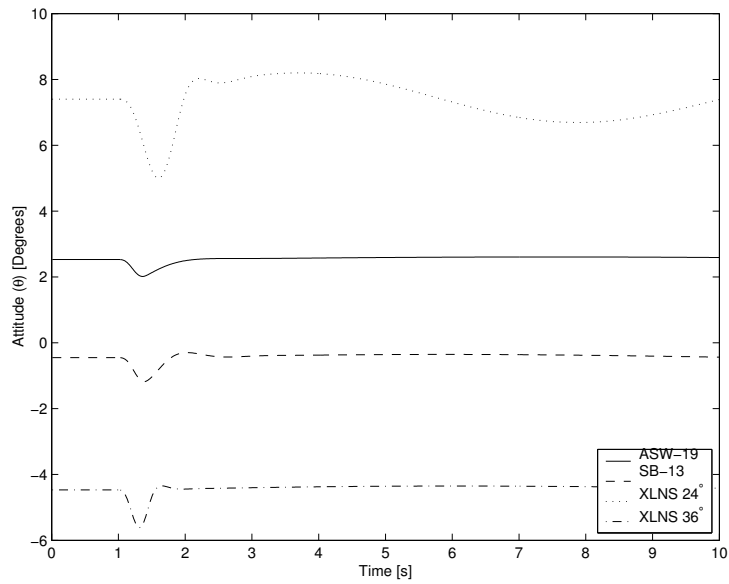
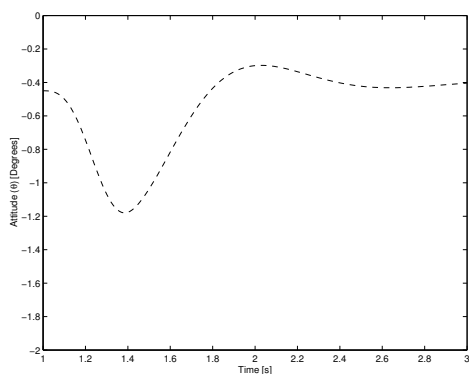
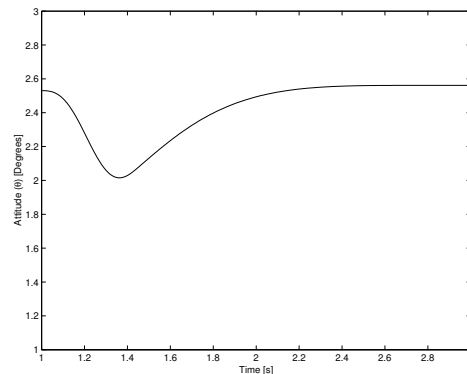


Figure 6.2: The response in aircraft attitude (θ) to a $1 - \cos$ gust, for the ASW-19, the SB-13, the 24° (15% static margin) and the 36° (5% static margin) sweep Exulans.

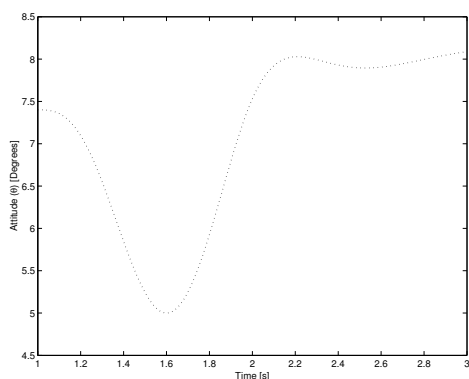
static margin at these sweep angles. The 30° sweep case has a 2% static margin. It has a strongly damped short period mode like the ASW-19 and the Cherokee. The 30° case has low static margin (2%) while the other cases have high static margin (10%). Since the low static margin case has a time response similar to those aircraft with favourable gust handling qualities, it is concluded that the Exulans has improved gust handling qualities at low static margins.



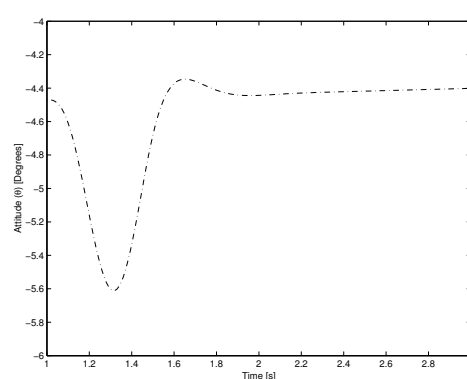
(a) SB-13.



(b) ASW-19.



(c) Exulans 24° sweep and 15% static margin.



(d) Exulans 36° sweep and 5% static margin.

Figure 6.3: Aircraft attitude (θ) to a $1 - \cos$ gust, during the period of the introduction of the gust, for the ASW-19, the SB-13 and Exulans.

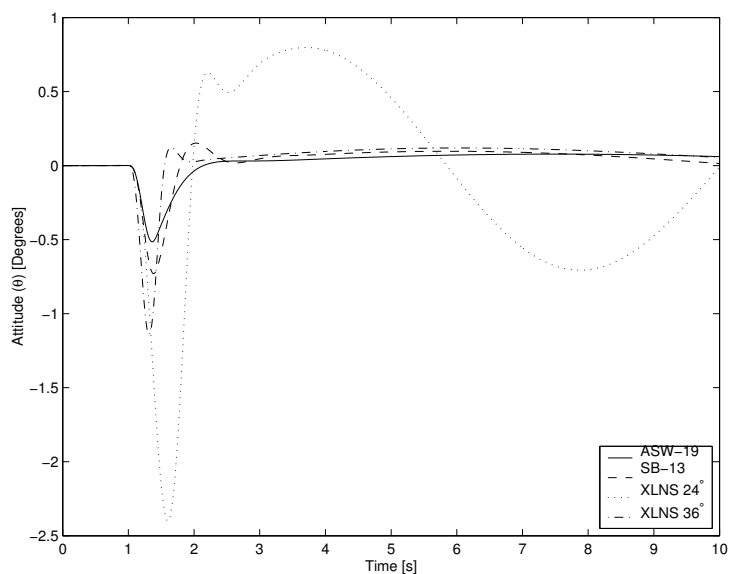


Figure 6.4: The superimposed response in aircraft attitude (θ) to a $1 - \cos$ gust, for the ASW-19, the SB-13, the 24° (15% static margin) and the 36° (5% static margin) sweep Exulans.

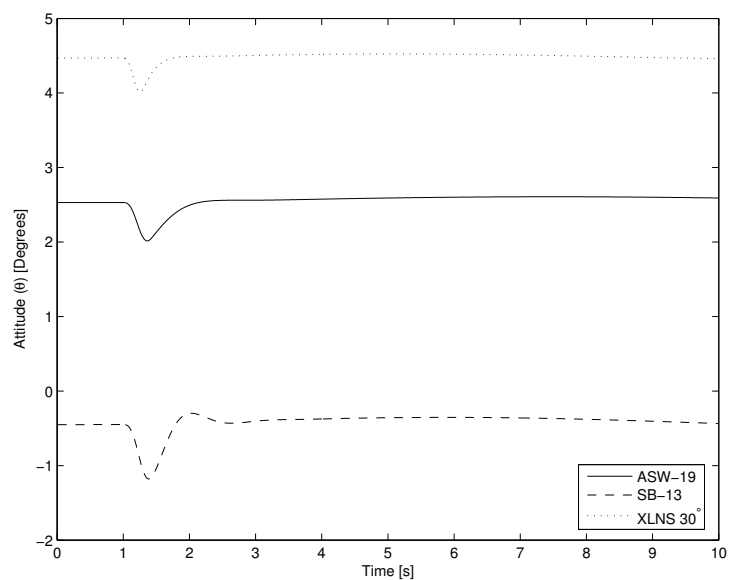
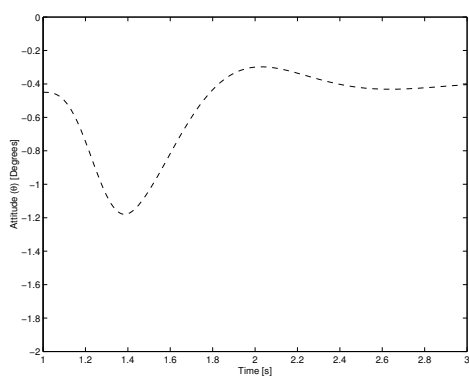
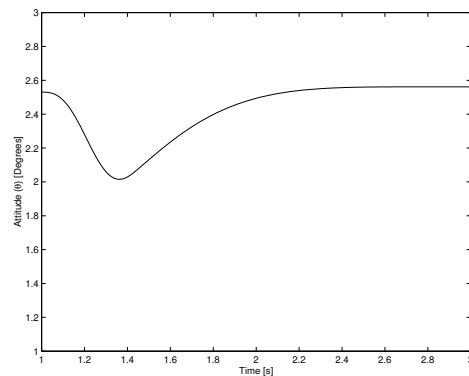


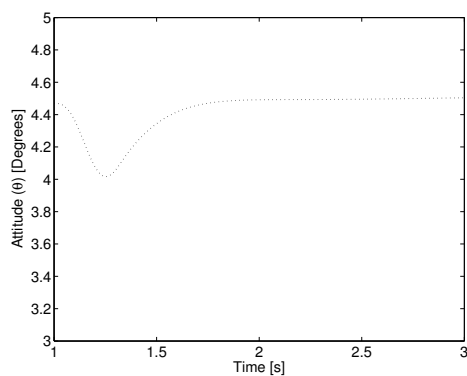
Figure 6.5: The response in aircraft attitude (θ) to a $1 - \cos$ gust, for the ASW-19, the SB-13 and the 30° (2% static margin) sweep Exulans.



(a) SB-13.



(b) ASW-19.



(c) Exulans 30° sweep and 2% static margin.

Figure 6.6: Zoomed aircraft attitude (θ) to a $1 - \cos$ gust, for the ASW-19, the SB-13 and Exulans.

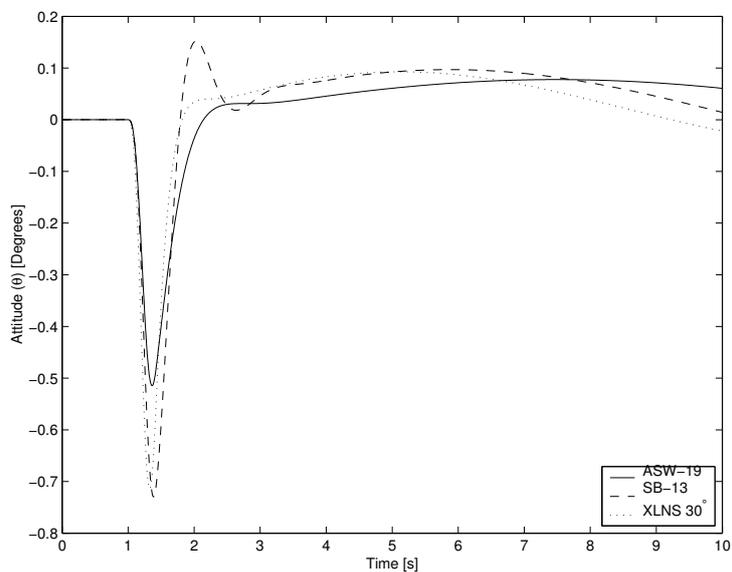


Figure 6.7: The superimposed response in aircraft attitude (θ) to a $1 - \cos$ gust, for the ASW-19, the SB-13 and the 30° (2% static margin) sweep Exulans.

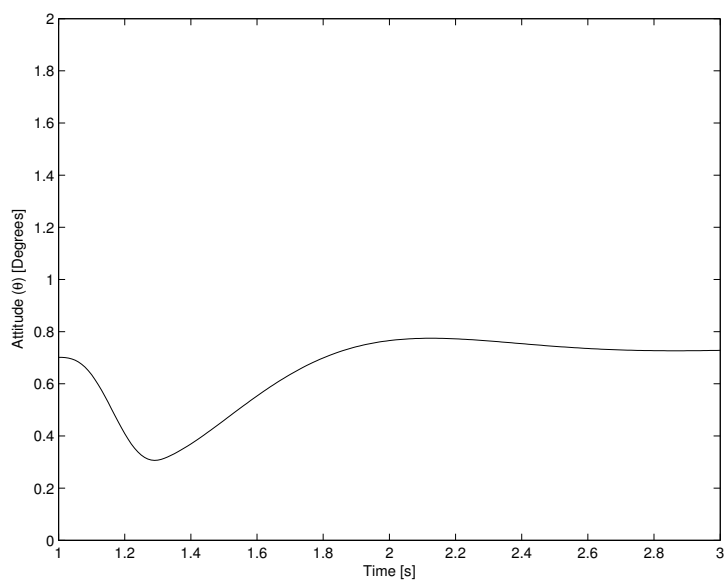


Figure 6.8: The response in aircraft attitude (θ) to a $1 - \cos$ gust, for the Piper Cherokee (gliding flight).

Chapter 7

Frequency Domain Analysis

Many of the analysis techniques listed in Chapter 3 are frequency domain techniques. The gull-wing configuration (with the Exulans as example) handling qualities were analysed by using these techniques. The results are presented here.

7.1 Thumbprint Criterion Analysis

The thumbprint criterion analysis methodology is presented in Section 3.3. This methodology was applied to the Exulans.

The handling qualities of different cases of sweep and static margin of the gull-wing configuration were investigated with the thumbprint analysis method. The cases were numbered for ease of reference. The numbering system is presented in Table H.2 of Appendix H. Different cases of sweep angle and static margin were investigated with the thumbprint criterion. The aerodynamic damping was kept at the baseline value for all cases. The ‘baseline’ values are defined as the parameter values presented in Section 4.7. The analysis was performed at four different values of static margin for the following cases:

- 20° outboard wing sweep (configurations 3, 6, 9, 12).
- 24° outboard wing sweep (configurations 15, 18, 21, 24).

- 30° outboard wing sweep (configurations 27, 30, 33, 36).
- 36° outboard wing sweep (configurations 39, 42, 45, 48).

The damping ratios and natural frequencies of the short period mode of the different cases were calculated by means of eigenvalue analysis (see Appendix B) and plotted on the short period opinion contours (the ‘thumbprint’ graph) of O’Hara (1967).

A typical result of the eigenvalue analysis is shown in Figure 7.1. The remainder of the results are included for reference purposes in Appendix J.1. The pilot opinions of different short period regions are shown as text labels. The short period natural frequencies and damping ratios of three configurations are plotted as circles. The number of each case or configuration (according to Table H.2) is shown as a text label next to the circle. The region of best handling qualities is indicated with a diamond shape on the plot. The damping ratio of the phugoid mode is also included on the plot, next to the aircraft configuration number.

Configurations 3, 6 and 15 are statically unstable. As a result of this, the thumbprint criterion cannot be applied to these cases. These configurations have to be analysed by means of another method such as the Neal-Smith method or a pilot in the loop simulation.

The thumbprint analysis results (Figure 7.1 and Figures J.1 to J.3) show that the Exulans will have the most favourable handling qualities at low static margins and at low sweep angles. From these results, it can be observed that configurations 9 and 18 are closest to the most favourable point on the thumbprint graph. These configurations have low static margin and wing sweep. Configurations 27 and 39 (see Figures J.2 and J.3) do not have good handling qualities according to the thumbprint criterion, but these cases have more favourable handling qualities than the other, higher static margin cases presented on the same graphs. The thumbprint analysis indicated that the high sweep and high static margin cases of the Exulans will be prone to pilot induced oscillation or *PIO*.

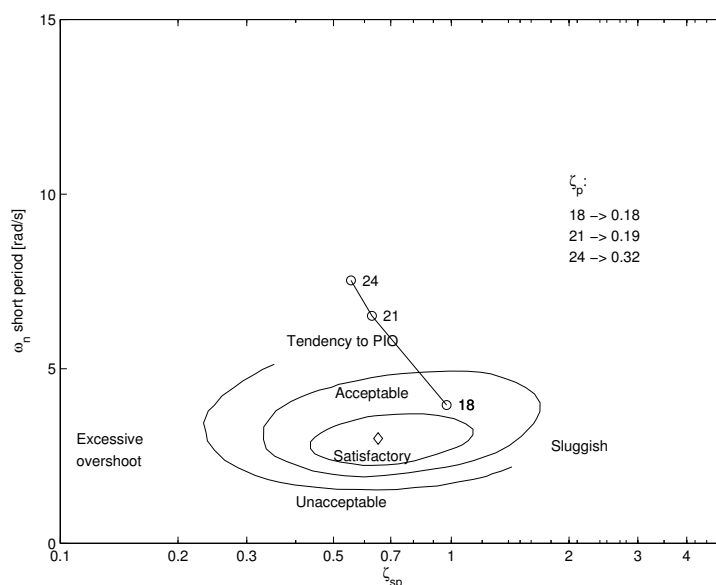


Figure 7.1: Thumbprint analysis for 24° outboard wing sweep, at various static margin cases, with the baseline aerodynamic damping. (Configuration nr. 18 is 24° 5% d, Configuration nr. 21 is 24° 10.7% d, Configuration nr. 24 is 24° 15% d, as per Table H.2)

7.2 Military Flying Qualities Specifications

Flying quality requirements are presented in MIL-F-8785C (1980). The methodology of the Military Flying Qualities analysis is presented in Section 3.4. The cases of the Exulans used for the thumbprint analysis were also analysed by means of the Military Flying Qualities analysis.

The results of the analysis are presented in Figure 7.2 and Figures J.4 to J.6.

The military flying qualities criteria require that the phugoid damping ratio $\zeta_p \geq 0.04$ for Level 1 flying qualities. This requirement was presented on the first line of Table 3.1. The phugoid damping ratio was presented as text on the graphs in Figure 7.1 and Figures J.1 to J.3. Configuration 18, for example has a phugoid damping ratio of 0.18 according to Figure 7.1. This is larger than the required minimum of 0.04. All the other Exulans cases that were investigated have phugoid damping ratios larger than 0.04 and therefore

satisfy Level 1 flying qualities with respect to this requirement.

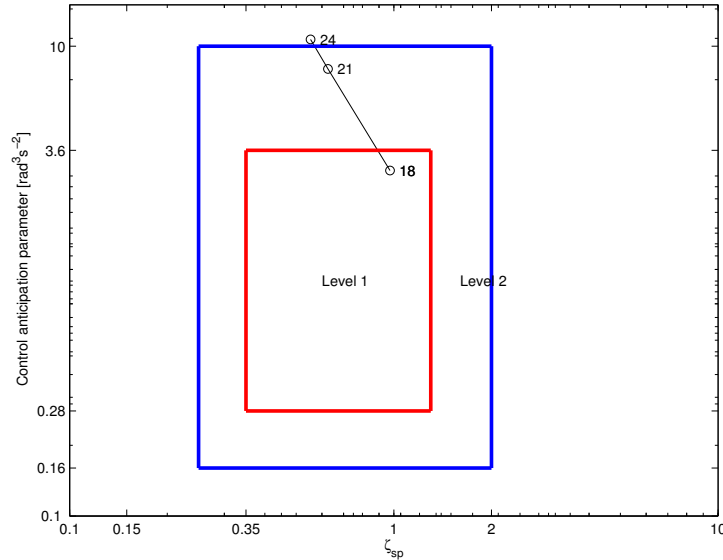


Figure 7.2: *CAP* for 24° outboard wing sweep, at various static margin cases, with the baseline aerodynamic damping. (Configuration nr. 18 is 24° 5% d, Configuration nr. 21 is 24° 10.7% d, Configuration nr. 24 is 24° 15% d, as per Table H.2)

Configuration 18 had Level 1 qualities with respect to the *CAP*. This configuration had ‘acceptable’ handling qualities according to the thumbprint criterion (see Figure 7.1). All other configurations had Level 2 flying qualities. This means that these configurations will have adequate flying qualities, with some increased pilot workload when compared to configuration 18.

When examining Figure 7.2 it can be observed that configuration 18 has better flying qualities than configuration 24, since the former is further away from the centre of the Level 1 bounding box. This indicates that lower static margins have more favourable handling qualities, since configuration 18 has a lower static margin than 21 or 24. The same trend can be observed with respect to wing sweep angle. The higher the wing sweep angle becomes, the poorer the handling qualities become. These results agree with the thumbprint analysis.

7.3 Shomber-Gertsen Analysis

This analysis method is presented in Section 3.6. The strength of the Shomber-Gertsen analysis method is that the handling qualities of an aircraft can be analysed at different airspeeds.

The different cases of Section I.1 of the pitch control input simulations were analysed using the Shomber-Gertsen method and the numbering system presented in Tables H.1 of Appendix H was used.

In order to vary the value of n_α , the above-mentioned cases were analysed with varying true airspeed (V) values. The speed was varied by 20% above and below the design trim speed.

Sample results from the analysis are presented in Figures 7.3 and 7.4. The remainder of the results are presented in Appendix J.3. The following observations (grouped per case set) can be made from the results of the analysis:

Group one (Static margin variations, 30° sweep, baseline aerodynamic damping, baseline control authority or Configurations 81, 90, 99, 108). The low speed case and the design speed had a $n_\alpha < 15$ g/rad and the high speed case had a $n_\alpha > 15$ g/rad. The cases with $n_\alpha < 15$ g/rad had acceptable to satisfactory handling characteristics. The cases with $n_\alpha > 15$ g/rad had unsatisfactory handling qualities. This indicates that speeds higher than the design speed will potentially have unsatisfactory handling qualities according to the Shomber-Gertsen method. This must be viewed as a serious flight limitation for the Exulans.

Group two (Static margin variations, 24° sweep, baseline aerodynamic damping, baseline control authority or Configurations 45, 54, 63, 72). No speed had a $n_\alpha > 15$ g/rad. Configurations 54, 63 and 72 has satisfactory to acceptable handling qualities. Configuration 45 (statically unstable case) could not be positioned on the contour map and therefore has unacceptable characteristics.

Group three (Static margin variations, 36° sweep, baseline aerodynamic damping, baseline control authority or Configurations 117, 126, 135,

144). All configurations and speeds that were investigated have unsatisfactory handling characteristics according to the design speed and the high speed case. The 'lower than design speed' case has satisfactory handling qualities for all cases.

Group four (Control authority variations, 30° sweep, baseline aerodynamic damping, 10.7% static margin at 30° or Configurations 93, 96, 99). The low speed case and design speed case had values of $n_\alpha < 15$ g/rad and the high speed case had a $n_\alpha > 15$ g/rad. Design speeds and low speeds displayed acceptable handling characteristics. The high speed case had unacceptable handling qualities. The control authority variations had a small impact on handling characteristics. This means that a 20% accuracy on the prediction of the control authority is sufficient for this handling quality analysis, since the effect of prediction errors on the result is small.

Group five (Control authority variations, 24° sweep, baseline aerodynamic damping, 10.7% static margin at 30° or Configurations 57, 60, 63). The design speed and the low speed case had $n_\alpha < 15$ g/rad with satisfactory handling qualities. The high speed case had a $n_\alpha > 15$ g/rad with unacceptable handling qualities. Once again, the control authority variation had a small effect.

Group six (Damping variations, 30° sweep, 10.7% static margin at 30°, baseline control authority, or Configurations 97, 98, 99). The design speed, the low speed case and the high speed case for configurations 98 and 99 had $n_\alpha < 15$ g/rad. Configuration 97 had $n_\alpha < 15$ g/rad for the low speed case and the design speed case, while the high speed case had a $n_\alpha > 15$ g/rad. Design speed cases and low speed cases all display acceptable handling qualities. Only the high speed case coupled with low damping displayed unacceptable handling qualities. The 20% variation in aerodynamic damping has an influence on the outcome of the handling quality study, but the effect is not so significant that it can change the pilot opinion. The airspeed is a much more significant

parameter with respect to handling qualities.

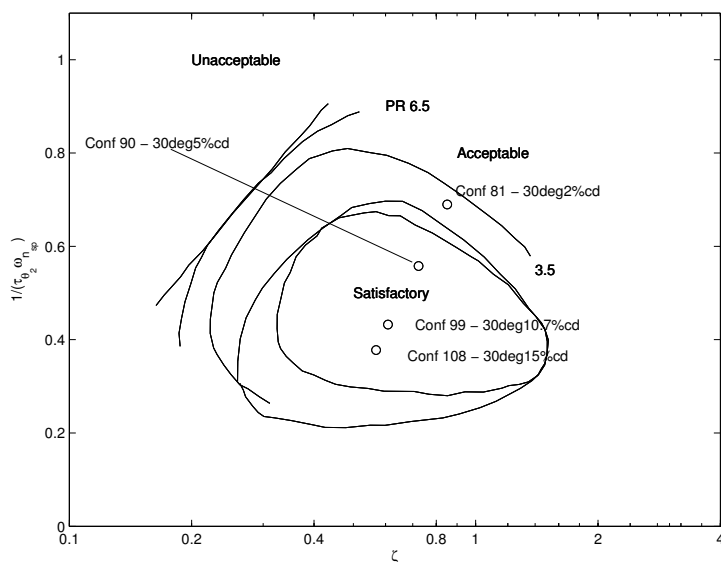


Figure 7.3: Group one analysis results for $n_\alpha < 15$ g/rad.

It may seem from the discussion in the previous paragraphs that there is a discontinuity between the results for $n_\alpha < 15$ and the results for $n_\alpha \geq 15$. It must however be remembered that handling qualities transition smoothly from acceptable to poor and that this discontinuity somewhat artificial because it is a result of how the handling quality criterion was defined in Shomber & Gertsen (1967).

The following conclusions can be drawn from the observations of the results:

- The estimation error of aerodynamic damping and control authority have an influence on handling quality predictions. A 20% variance in these parameter values will however not alter the conclusions of the handling quality study, since the effect is small enough.
- Speeds higher than the design trim speeds show a tendency to result in unacceptable handling qualities for the case of the Exulans. It follows as a recommendation that the Exulans should not be operated at speeds

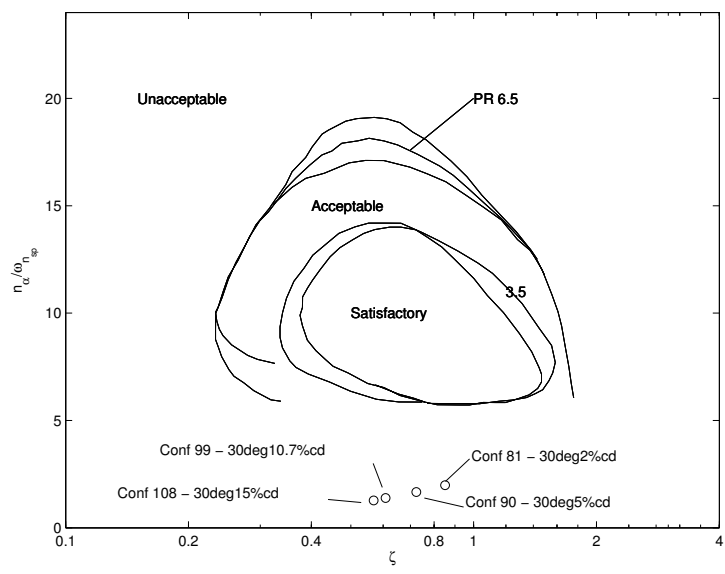


Figure 7.4: Group one analysis results for $n_\alpha \geq 15$ g/rad.

higher than the design speed (for a given sweep angle) as a risk reduction measure.

7.4 Neal-Smith Handling Qualities Analysis

The Neal-Smith analysis method is presented in Section 3.7. This method was applied to the Exulans. The Exulans configurations that were investigated in the pitch control step input analysis (see Section I.1) were also used as subjects for the Neal-Smith analysis. The Neal-Smith analysis was performed at the design airspeeds for each of the sweep cases that were analysed.

The results of the Neal-Smith analysis are presented in Figure 7.5.

The following conclusions can be drawn from the results:

- Most of the configurations that were investigated fall within the boundaries of favourable pilot opinion. The pilot rating for all these configurations are 3.5 or better. The exceptions are the statically unstable configurations (such as 24° sweep case with a 2% static margin at 30°). The Neal-Smith method indicated that the human pilot model with a 0.3s time delay could not compensate or control negative static margin cases. Since the statically unstable configurations did not achieve the minimum bandwidth criterion, it cannot be plotted on the Neal-Smith chart. This chart is only defined for configurations that achieve the compensation criterion.
- All the configurations that were investigated required lead compensation to achieve the bandwidth and droop criteria.
- The variation of $C_{M_{\delta_e}}$ of 20% with respect to the baseline had a very small impact on handling qualities. The estimation error of this parameter is therefore not a critical factor with respect to handling qualities. The methods used to estimate this parameter are therefore judged to be sufficiently accurate for the application.
- The analysis performed on configurations 97, 98 and 99 indicate that the 20% variation in damping due to estimation error has a small effect on the Neal-Smith opinion rating.
- The Neal-Smith analysis showed that the gull-wing configuration will

have good handling qualities for a wide range of sweep and static margin in calm conditions.

The Neal-Smith method is important because it provides a way to assess the effect of control authority and the pilot-in-the loop on handling qualities. The fact that a simulated pilot in the form of a transfer function model is used, is advantageous because it offers repeatability, where true pilot-in-the-loop analysis and simulation is never completely repeatable.

The pitch stick force gradient of the Exulans was taken as 25 N/g for the analyses performed. This value was obtained from Neal & Smith (1970). This stick force gradient was an initial assumption, since the aircraft was not constructed at the time of completion of this study. It must be investigated further and optimised for the case of the Exulans in a future study.

Bandwidth is a very important parameter with respect to pilot opinion in this method. When a pilot manoeuvres the aircraft very aggressively, more bandwidth is required compared to scenarios where more gradual manoeuvres are executed. The gull-wing configuration was evaluated with a bandwidth requirement of 3.5 rad/s. This was done because the Neal-Smith opinion chart was set up using this bandwidth requirement. The second reason for using 3.5 rad/s is because the gull wing planform aircraft might be used for aerobatic flying purposes, where higher bandwidth is required due to rapid flight manoeuvres. If the bandwidth criterion is relaxed, the configurations that showed unacceptable characteristics at high bandwidth, would show more acceptable handling characteristics.

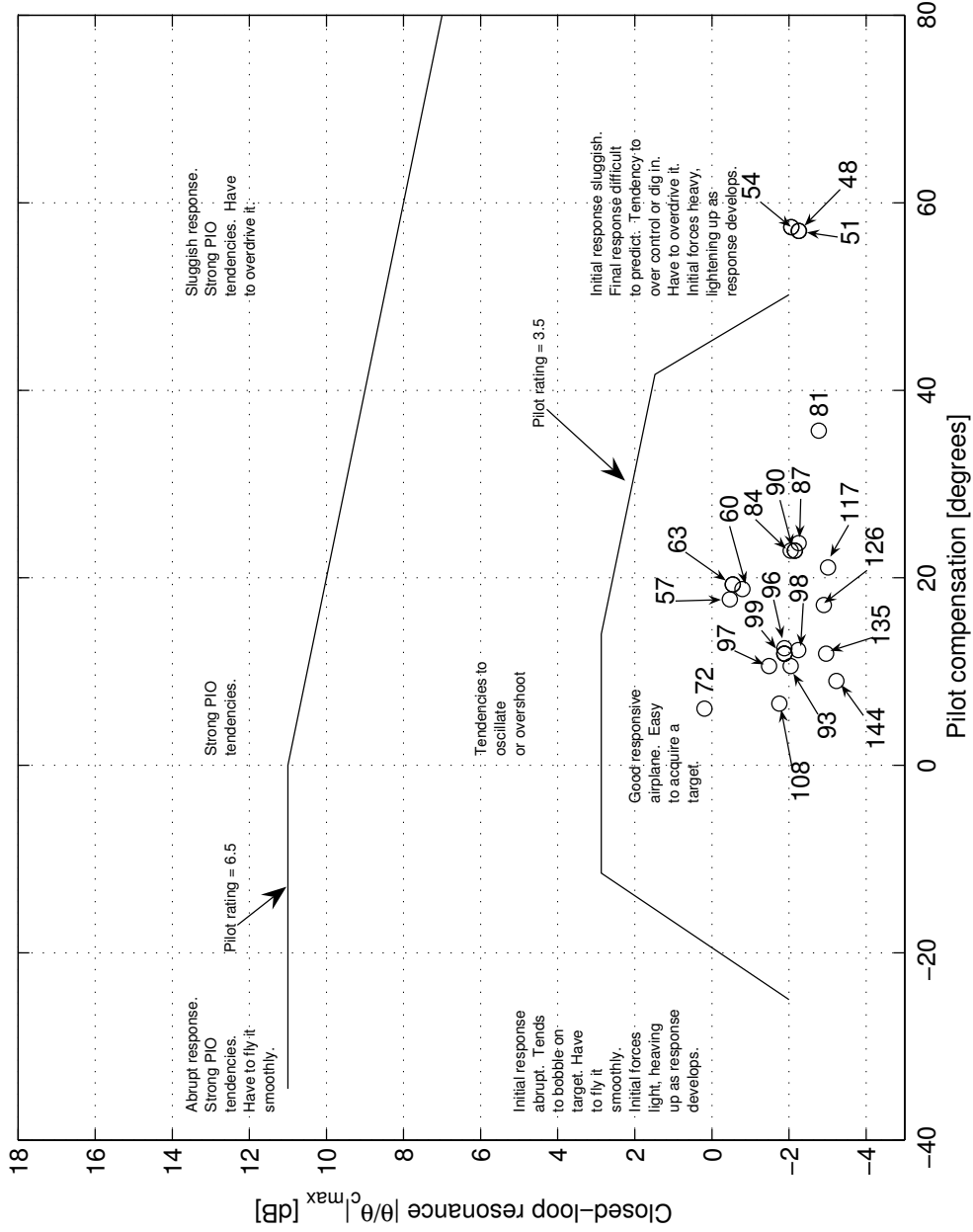


Figure 7.5: Results of the Neal-Smith study performed on various gull-wing configurations.

7.5 Frequency Domain Analysis Summary

Many important conclusions were drawn in this chapter regarding the handling qualities of the gull-wing configuration. Several analysis methods were used to predict handling qualities. The different methods are suitable for evaluating different aspects of handling qualities. Certain methods contradict each other and therefore an overview summary is required:

- The Military flying qualities criteria and the thumbprint analysis are useful for evaluating the inherent (raw) aircraft dynamics. These results indicated that the raw aircraft has some unpleasant characteristics, but that the handling qualities improve as static margin is decreased. These methods cannot evaluate marginally stable or unstable configurations.
- The Shomber Gertsen analysis is useful for evaluating handling qualities at different trim speeds. Airspeed is an important parameter in the zeros of the aircraft pitch transfer function. The zeros of the transfer function have an important influence on handling qualities. This method seems to indicate that the gull-wing handling qualities are generally acceptable, but not at speeds above the design trim speed.
- The Neal-Smith analysis is the most complete of all the methods used to evaluate the handling qualities. This method includes the stabilising effect of the pilot and is useful for the evaluation of marginally stable aircraft cases. It is also useful for preliminary pilot-in-the-loop studies and for evaluating the effect of varying control authority. The Neal-Smith results indicate that almost all the Exulans cases have good handling qualities, except for the marginally stable and unstable cases. This means that the CG region for acceptable handling qualities stops forward of the neutral point for the gull-wing configuration. The Neal-Smith method takes into account the stabilising effect of the pilot and as a result, its results should be used in preference to the less complete thumbprint and Military criteria.

- The C-star results of Chapter 6.1 predicts that the Exulans will have poor handling qualities for rapid manoeuvring and during landings. This contradicts the Neal-Smith results. When the two methods are compared it is evident that the stabilising effect of the pilot is not taken into account with the C-star method. Neal & Smith (1970) also states that the C-star method does not always correctly predict handling qualities. It is concluded that the Neal-Smith analysis results should rather be used since it is a more thorough method and because it has also been properly benchmarked (see Neal & Smith (1970)), whereas the C-star method is a mathematical method based on a summary of different studies (Tobie et al., 1966).
- The effects of control authority and damping variations on handling qualities were investigated. This investigation was required due to the presence of estimation errors in calculating these parameter values. The results indicated that these variations do not have a significant influence on handling qualities. It is concluded that the accuracy with which these parameters were estimated was sufficient.

In summary the Exulans should exhibit satisfactory handling qualities for a wide envelope of wing sweep and static margin, except at speeds higher than the design trim speed.

Chapter 8

Turbulence and Tumbling Criteria

Tailless aircraft have low pitch inertia and aerodynamic damping when compared to conventional aircraft. These characteristics cause tailless aircraft to have unique characteristics during gusty or turbulent conditions. Tailless aircraft are also more susceptible to tumbling than tailed aircraft for these reasons. Some special handling qualities criteria have been developed to analyse tailless aircraft with respect to gusty conditions and tumbling. These criteria were applied to the gull-wing configuration. The results are presented here.

8.1 Turbulence Handling Criterion

Some tailless aircraft have been known to display unfavourable handling characteristics in turbulent conditions. The unfavourable handling characteristics are associated with the pitching phenomenon of ‘pecking’. Examples of aircraft that are prone to this condition are the SB-13, the Horten H XV b and H XV m (Nickel & Wohlfahrt, 1994:104).

The work of Mönnich & Dalldorff (1993) investigated the handling qualities of flying wings in turbulent conditions. The SB-13 handling qualities were investigated and compared to a modern conventional sailplane, the ASW-19.

A tailless aircraft handling criterion (hereafter referred to as the Mönlich-Dalldorff criterion) for turbulent conditions was derived in the study. This was applied to the gull-wing configuration. The Mönlich-Dalldorff analysis was repeated in this study and the same results were achieved as documented in Mönlich & Dalldorff (1993).

The Mönlich-Dalldorff criterion states that a tailless aircraft (or any aircraft for that matter) shall have favourable handling qualities in turbulent conditions provided that the following inequality is satisfied for that particular aircraft:

$$\frac{C_{M_\alpha}}{C_{M_q}} < (C_{L_\alpha} + C_{D_e}) \frac{\rho S \bar{c}}{2m} \quad (8.1)$$

The variables of the inequality are defined in the nomenclature list. If the inequality of Equation 8.1 is satisfied, the existence of a zero of the gust velocity to pitch attitude transfer function in the left half plane is guaranteed. The left half plane zero leads to favourable gust handling qualities. The inequality is true for almost all conventional aircraft, but this is not the case for all flying wing aircraft.

The Mönlich-Dalldorff criterion was applied to various static margin and sweep cases of the gull-wing configuration. The criterion was evaluated for air density values of 1.225 kg/m³ and 0.855 kg/m³. These density values correspond to sea level and an altitude of 12000 ft for the International Standard Atmosphere. The sea level altitude was chosen to represent the case of wake turbulence from an aerotow at sea level, while the upper altitude limit represents the maximum safe altitude without an oxygen supply on board. The aircraft parameters used in the evaluation were taken from Table 4.4. The trim lift C_L and equilibrium drag (C_{D_e}) were calculated using an angle of attack of 9.8° for 24° sweep, 4.1° for 30° sweep and 2.1° for 36° sweep for the gull wing planform aircraft. The parameter values mentioned were substituted into Equation 8.1 and the results are presented in Tables 8.2 to 8.5. The trim conditions used for the analysis are presented in Table 8.1. The result tables contain some of the parameters of the investigation as well as the numerical values of the left- and right hand side of the inequality of Equation 8.1. If

the right hand side value is larger in magnitude than the left hand side, the particular configuration will have satisfactory turbulent condition handling qualities. The analyses showed that the ratio of the moment curve slope and the aerodynamic damping coefficient had the most significant influence on the inequality of the Mönlich-Dalldorff criterion.

Table 8.1: Trim conditions used for the Mönlich-Dalldorff analysis of the gull-wing configuration.

Sweep ($\gamma, ^\circ$)	$\alpha, ^\circ$	C_L	C_{L_α}	C_{D_e}
24	9.78	0.954	5.232	0.040
30	4.13	0.430	5.146	0.019
36	2.12	0.244	5.031	0.016

Table 8.2: The evaluation of the Mönlich-Dalldorff criterion for different out-board wing sweep angles of the gull-wing configuration aircraft for a 2% static margin at 30° sweep case.

Sweep ($\gamma, ^\circ$)	C_{M_α}	C_{M_q}	Left	Right	Right
				Sea level	12000 ft
24	0.148	-1.218	-0.121	0.247	0.172
30	-0.103	-2.035	0.051	0.242	0.169
36	-0.365	-3.097	0.118	0.236	0.165

The results (Tables 8.2 to 8.5) indicate that the turbulent handling qualities become less favourable with higher sweep angles. As the sweep angle increases, the left hand side of the inequality starts getting closer in magnitude to the right hand side. The results also show that turbulent handling qualities deteriorate with altitude. Table 8.4 indicates that the right hand side (12000 ft column) of the equation is less than the left hand side of the equation for all sweep angles of the 10.7% static margin (at 30° sweep) case. In contrast, the sea level column shows the right hand side to be larger for all sweep cases.

The inequality is favourable with respect to the Mönlich-Dalldorff criterion for most sweep angle and static margin configurations of the gull-wing

Table 8.3: The evaluation of the Mönlich-Dalldorff criterion for different out-board wing sweep angles of the gull-wing configuration aircraft for a 5% static margin at 30° sweep case.

Sweep (γ , °)	C_{M_α}	C_{M_q}	Left	Right	
				Sea level	12000 ft
24	-0.011	-1.365	0.008	0.247	0.172
30	-0.257	-2.204	0.117	0.242	0.169
36	-0.518	-3.291	0.157	0.236	0.165

Table 8.4: The evaluation of the Mönlich-Dalldorff criterion for different out-board wing sweep angles of the gull-wing configuration aircraft for a 10.7% static margin at 30° sweep case.

Sweep (γ , °)	C_{M_α}	C_{M_q}	Left	Right	
				Sea level	12000 ft
24	-0.309	-1.693	0.182	0.247	0.172
30	-0.551	-2.546	0.216	0.242	0.169
36	-0.804	-3.695	0.217	0.236	0.165

configuration aircraft. This indicates that the aircraft will have satisfactory gust handling characteristics over a large region of the operational envelope. The configuration with a 24° sweep and 2% static margin (at 30° sweep) is statically unstable. This implies that the inequality is true by default since the left hand side of the expression then becomes negative. All sea level cases except for the ones having a 15% static margin (at 30° sweep) have favourable handling qualities according to the criterion. The 12000 ft cases of all the 2% and 5% static margin cases have favourable handling qualities and the higher static margin cases all have unfavourable characteristics.

The low static margin cases are most favourable with respect to gust handling qualities according to the criterion. This compares well with the results from the thumbprint criterion analysis presented in Section 7.1. This is because a lower pitch moment stiffness (that goes along with lower static margin) causes the left hand side of the inequality to be smaller in magnitude. This causes the inequality of the criterion to be true. It may be

Table 8.5: The evaluation of the Mönlich-Dalldorff criterion for different out-board wing sweep angles of the gull-wing configuration aircraft for a 15% static margin at 30° sweep case.

Sweep (γ , °)	C_{M_α}	C_{M_q}	Left	Right	
				Sea level	12000 ft
24	-0.531	-1.980	0.268	0.247	0.172
30	-0.772	-2.895	0.267	0.242	0.169
36	-1.018	-4.051	0.251	0.236	0.165

concluded that the gull-wing configuration's ratio of pitching moment stiffness to aerodynamic damping is favourable with respect to gust handling qualities.

8.2 Tumbling

An aircraft can inadvertently enter an out-of-control tumbling motion under certain conditions. Tumbling can be defined as an autorotative pitching motion primarily about an axis parallel to a vehicle's lateral axis, plus translation in a vertical plane along an inclined flight path. This is a very serious condition that may lead to the loss of the aircraft. Tumbling may be caused by high pitch rates and conditions where an aircraft has entered a 'tail slide' (Fremaux & Vairo, 1995). A tail slide is entered when the air over the wing travels from the aft end of the aircraft to the front of the aircraft. A tail slide can therefore occur during stalls and violent spins.

The data of Fremaux & Vairo (1995) will be used to analyse the gull-wing configuration with respect to tumbling. The mentioned paper is the result of wind tunnel work that was used to identify the driving parameters of the tumbling phenomenon on tailless aircraft. The mechanisms of tumbling were also investigated in that study. No forward/backward swept (gull-wing configuration) models were tested in the study and hence the results from the evaluation should not be view as directly applicable to the gull-wing. The test models used are presented in Figure 8.1. In the absence of more appli-

cable wind tunnel data, this data may be relevant to provide a first order estimate assessment of tumbling behaviour. Fremaux & Vairo (1995) found that positive static stability does not necessarily preclude tumbling. Factors that influence tumbling are centre of gravity location, mass distribution and geometric aspect ratio. This study created a chart that indicates the combinations of static margin and aspect ratio that are likely to lead to tumbling tendencies with an aircraft.

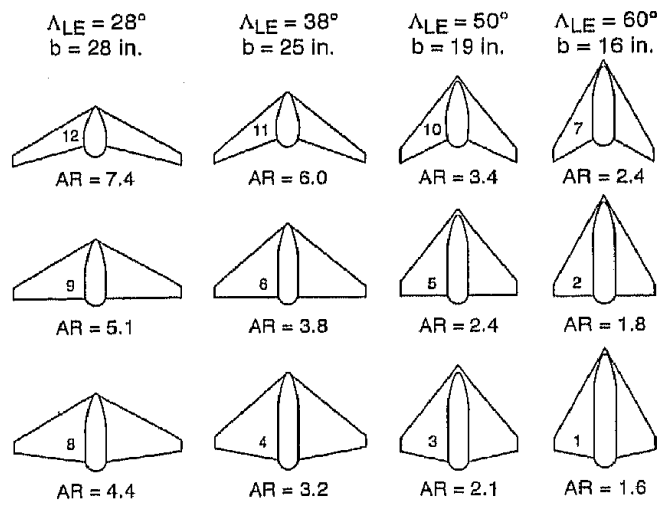


Figure 8.1: Generic flying wing models used for tumbling research. (Fremaux & Vairo, 1995)

Tumbling happens when $I_{xx} > I_{yy}$ ('wing-heavy' as Fremaux & Vairo (1995) refers to it) and when the aircraft static margin and aspect ratio falls within the boundaries as described in Figure 8.2.

Tailless aircraft are most likely to tumble while conventional configurations are the least likely to tumble. (Fremaux & Vairo, 1995) With this in mind, it is important to investigate whether the gull-wing configuration is also susceptible to this condition.

The gull-wing configuration under investigation has a high aspect ratio (12). It is expected that the aircraft will mostly be operated at low static margin (2 to 10%). The Exulans has an I_{xx} value of 585 kg·m². This means that the I_{xx} to I_{yy} ratio is at least larger than 13 (see Figure 4.5 for I_{yy} values

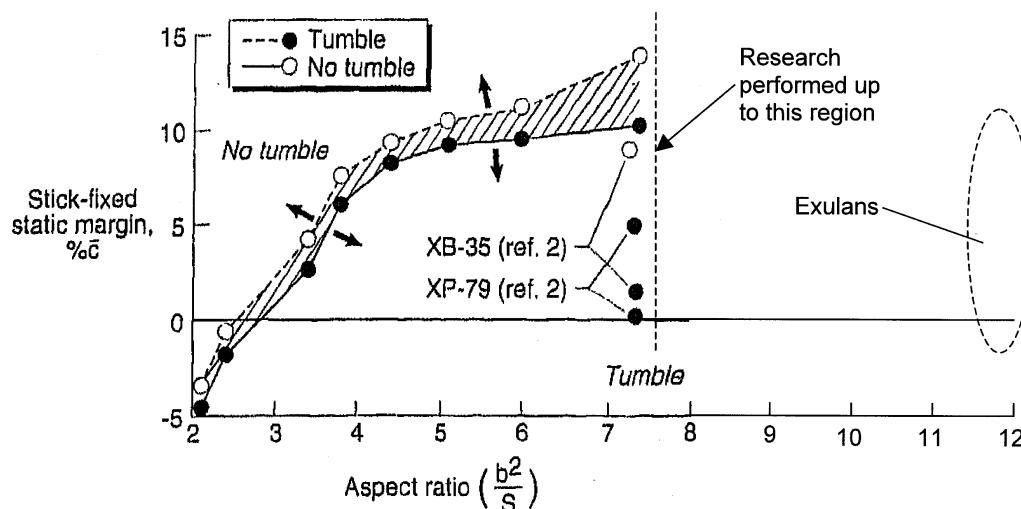


Figure 8.2: Static margin for tumbling as a function of aspect ratio for models with ‘wing-heavy’ (ie. $I_{xx} > I_{yy}$) loadings. (Fremaux & Vairo, 1995)

for the Exulans), depending on sweep angle. When these inertia ratios are compared to Figure 8.2 it can be concluded that the gull-wing configuration is likely to be susceptible to tumbling, assuming the trend can be extrapolated linearly to higher aspect ratios.

The tumbling research presented in Figure 8.2 was performed using thin flat plate wing models with a centre section to model the fuselage and acting as ballast. The research indicates that thick airfoil sections (Exulans has a thick airfoil section) have a tendency to be less susceptible to tumbling. Further research needs to be done on the gull-wing configuration’s tumbling tendencies because engine nacelles, canopies, and any protrusion might have an effect on tumbling (Fremaux & Vairo, 1995). It is suggested that a detailed aerodynamic analysis be performed on the Exulans to determine whether its thick wing sections, winglets and fuselage could prevent tumbling behaviour.

As an initial estimate, there exists reasonable concern that the gull-wing configuration might be susceptible to tumbling. It may also be concluded that manoeuvres that may cause tumbling (high pitch rates, stalls and spins) should be avoided with the gull-wing configuration.

Chapter 9

Handling Qualities and Performance

Tailless flight should be able to offer attractive fundamental benefits to aviation. Practical implementation has revealed several shortcomings which render the benefits significantly compromised. At the core of the challenge lies the efficiency deterioration which results from the quality of the lift distribution over the main wing. The main wing of a tailless aircraft is responsible for the stability and control function (this is performed by the empennage on a tailed aircraft). It is therefore unavoidable to find variations of the lift distribution during flight. Flight efficiency demands that the lift distribution be of good quality to minimise the loss of energy in the wake of flight. This loss is manifested in vorticity in the wake resulting from gradients in the lift distribution. It is classified as induced drag in the drag brake-down.

In order to unlock the potential benefits of tailless flight it becomes necessary to achieve acceptable stability and control properties with a minimum penalty on the induced losses. Stability and control must be investigated together with performance issues to ensure that handling qualities are not optimised at the cost of performance.

When a tailless aircraft's CG is placed on the E-point (the O-point if the tailless aircraft has winglets) and the wing is designed to have an elliptical lift distribution, the aircraft will have the best Oswald efficiency. The region

between the E-point and the O-point is shown as hatched in Figure 9.1. This hatched region is associated with the best Oswald efficiency. In accordance with the argument of the first paragraph of this chapter, the tailless design would benefit if this region of best Oswald efficiency would somehow overlap with good handling qualities.

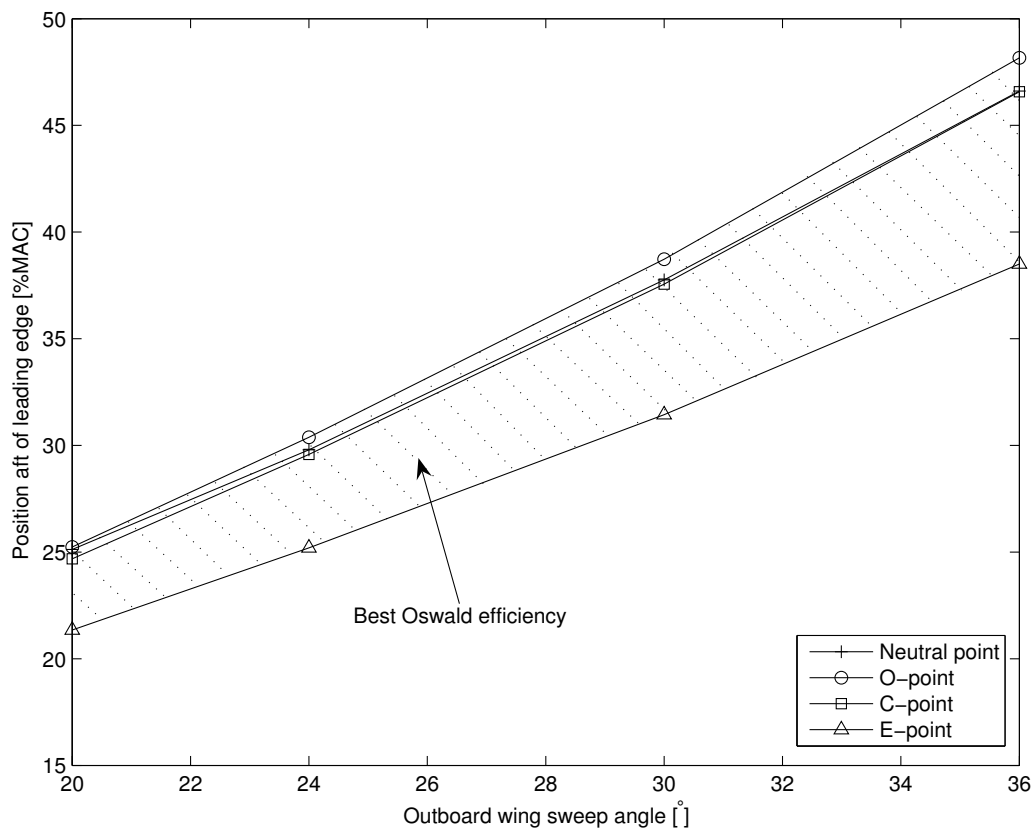


Figure 9.1: Region of best Oswald efficiency for the Exulans. The y-axis represents the distance behind the wing leading edge (at plane of symmetry).

A number of methods were used in Chapters 6 and 7 to evaluate the handling qualities. These methods were used to define a region of sweep and CG position with satisfactory (PR is 3.5 or better) handling qualities. Of these methods, the Neal-Smith method is the most complete method, since the dynamics of the pilot as a controller are not neglected. Compare

this to the thumbprint analysis that is more simplistic in nature. The pole analysis results ignore the contributions of the pilot and the zeros of the aircraft transfer function. The C^* method takes into account the effects of the aircraft poles and zeros. The C^* method is a time domain method and as such is also capable of handling a non-linear aircraft model. None of these methods investigate the effects of gusty conditions on handling qualities. The Mönlich-Dalldorff criterion was used to evaluate the gull-wing configuration with respect to turbulent conditions. Due to the strengths of the different analysis methods, a combination of all the analysis results was used to set up the boundaries of acceptable handling qualities in Figure 9.2.

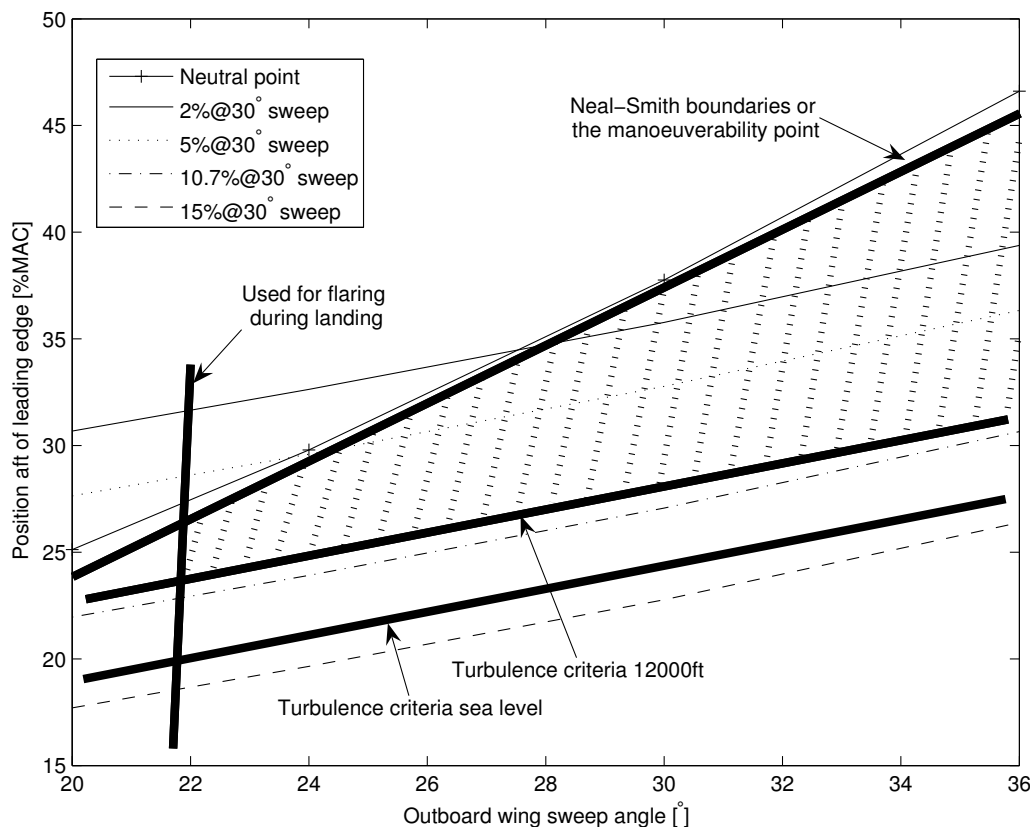


Figure 9.2: Region of acceptable handling qualities (PR is 3.5 or better) for the Exulans for different sweep angles and CG positions. The y-axis represents the distance behind the wing leading edge (at plane of symmetry).

Four lines in bold print are used to mark off the boundaries of acceptable handling characteristics in Figure 9.2. The line labelled ‘Used for flaring’ is used to mark off the low sweep angles. The handling qualities in this region were not investigated because these sweep angles are only used during the flare manoeuvre of landing and not during normal flight. The line used to mark off ‘Turbulence criteria’ was constructed by drawing a line parallel and just above the line of the 15%@30° sweep *CG* location function. This line represents the results of Section 8.1 where all *CG* locations indicated good gust handling qualities, except for the 15%@30° sweep *CG* location function. A similar line is used to indicate the region of good handling qualities at altitude. This is because gust rejection characteristics deteriorate with altitude. The fourth bold line on the graph represents the Neal-Smith results of Section 7.4. These results indicated that marginally stable and unstable configurations cannot be compensated by the average human pilot. The region of satisfactory handling qualities is hatched for purposes of clarity.

The four *CG* configurations investigated in this study are a function of outboard wing sweep and are specified as a percentage of mean aerodynamic chord at 30° wing sweep. The centre of gravity configurations are specified with respect to the static margin at 30° outboard wing sweep. 30° was chosen as a reference because the trim speed at this sweep angle is the cruise design speed. As an example, a legend caption in Figure 9.2 of ‘2%@30°’ indicates a *CG* configuration that has a static margin of 2% at 30° outboard wing sweep. At wing sweep angles lower than 30°, this configuration will have a static margin lower than 2% and at wing sweep angles higher than 30°, it will have a static margin higher than 2%. The four *CG* configurations cover a wide range of static margins and were chosen so that the minimum static margin that is represented is not less than -5.5%. All the quantities are plotted as distances referenced to the mean aerodynamic chord of the aircraft, measured from the leading edge of the wing of the aircraft on the plane of symmetry¹ of the wing. Since all the quantities are plotted on a scale referenced to the mean aerodynamic chord, the static margin for any configuration and sweep angle may be read off as the distance between

¹This is the position of $y=0$ on the body axis system described in Figure 4.1.

the CG for a particular configuration (at a particular sweep angle) and the neutral point at that sweep angle.

The regions for acceptable handling qualities and best Oswald efficiency have now been defined and in Figure 9.3 these two regions are superimposed. This figure shows that there is a significant overlap between the region of good performance and acceptable handling (the cross-hatched region).

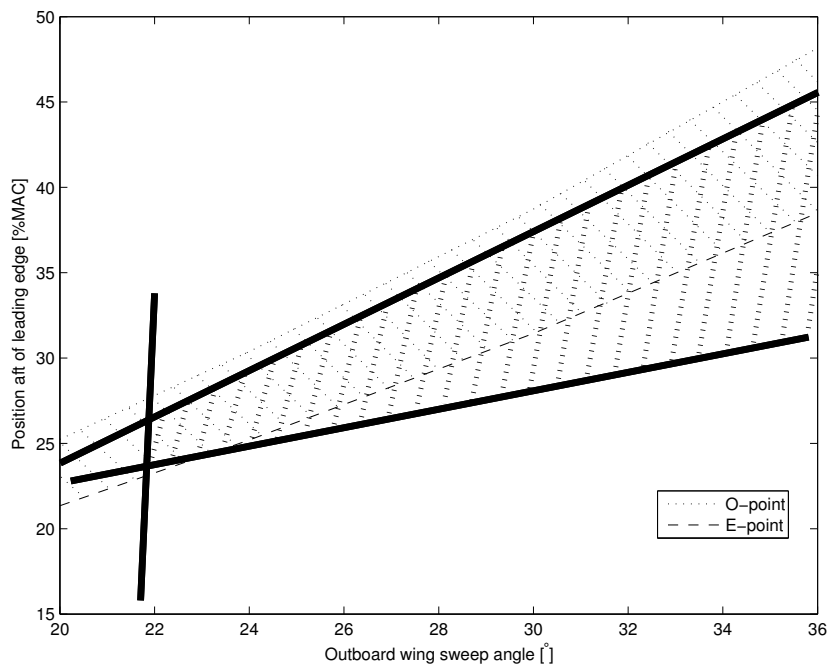


Figure 9.3: Superposition of regions of acceptable handling qualities and best Oswald efficiency for the Exulans. The y-axis represents the distance behind the wing leading edge (at plane of symmetry).

In Figure 9.4 the region of good handling and performance is presented together with the CG cases that were studied. Two of the configurations (2% at 30° and 5% at 30°) show a partial overlap with the favourable region. This represents the fundamental conclusion of this study:

A region of CG position and wing sweep exists for the gull-wing configuration that, given certain maximum speed constraints, the aircraft has satisfactory handling qualities in addition to the best Oswald efficiency.

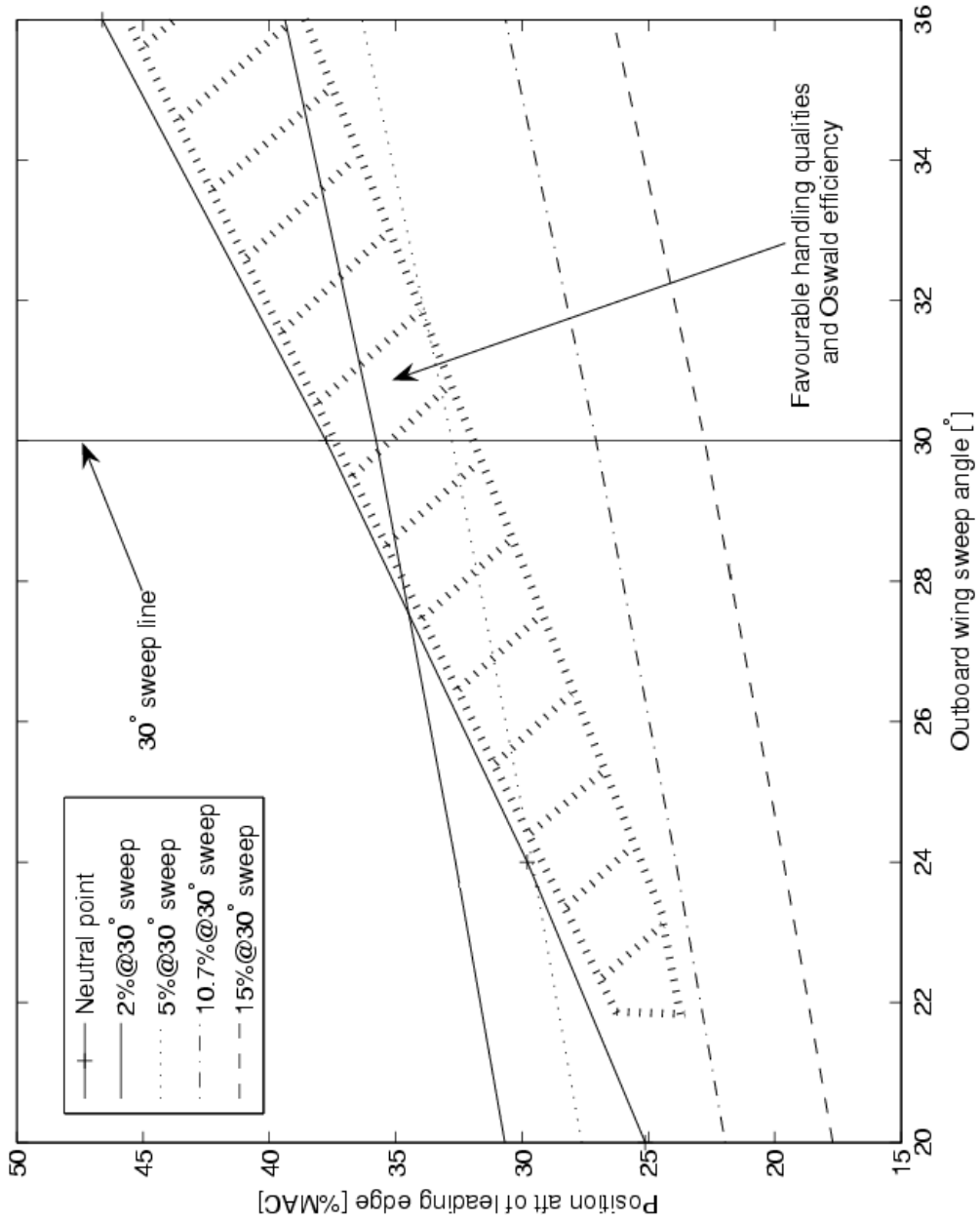


Figure 9.4: Region with both acceptable handling qualities and best Oswald efficiency for the Exulans. The y-axis represents the distance behind the wing leading edge (at plane of symmetry).

Chapter 10

Conclusion

A longitudinal handling quality investigation was performed on a tailless swept gull-wing configuration. An example of this type of aircraft is the Exulans that is under development at the University of Pretoria. The study assumed that lateral handling quality issues, such as tip stall and related spinning, will be handled in a separate study.

A mathematical model of the Exulans was created in order to investigate its pitch handling qualities. The handling qualities of the aircraft were evaluated using the mathematical model and methods obtained from literature.

In summary, the most important parameters that influence the handling qualities of the swept gull-wing configuration aircraft are static margin and the $\frac{C_{M\alpha}}{C_{Mq}}$ ratio.

The following conclusions were drawn from the handling quality investigation:

- A region of CG position and wing sweep exists for the gull-wing configuration that, given certain maximum speed constraints, the aircraft has satisfactory handling qualities in addition to the best Oswald efficiency.
- The handling qualities of the Exulans in gusty conditions should be acceptable if the aircraft has a favourable $\frac{C_{M\alpha}}{C_{Mq}}$ ratio. This ratio is acceptable with a static margin of below 5% (at 30°) together with an

aerodynamic damping coefficient of less than 3.2/rad (absolute value). Handling qualities in gusty conditions deteriorate with altitude, but is still acceptable at 12000 ft at low static margins. At low static margins, the short period mode of the aircraft is such that it has good disturbance rejection properties. This is a potential improvement on existing tailless designs that have exhibited poor disturbance rejection qualities.

- It is advisable to place the CG of the pilot as close as possible to the CG of the aircraft. A sitting pilot position with the ears of the pilot on the longitudinal aircraft CG position is optimal with respect to handling qualities. This type of pilot position has the effect of minimizing the magnitude of the pitch accelerations to which the pilot is subjected, which leads to improved handling qualities.
- The study indicated that the gull-wing configuration could be susceptible to tumbling. A gull-wing aircraft has a high aspect ratio and an unfavourable inertia ratio with respect to tumbling due to its geometry and mass distribution. Manoeuvres that may cause tumbling (high pitch rates, stalls and spins) should be avoided where possible with the gull-wing configuration.
- The Shomber-Gertsen handling qualities analysis showed that the Exulans will potentially have degraded handling qualities at true airspeeds above the design airspeeds. The Exulans is predicted to have satisfying handling qualities below and at the design speeds.
- The handling characteristics of the Exulans are insensitive to changes in pitch inertia that are within 10% from the baseline. This means that the handling qualities will not be sensitive to the placement of relatively large point masses such as batteries, as long as the CG of the aircraft is correctly placed.
- The variation of the $C_{M_{\delta_e}}$ and C_{M_q} parameters of 20% with respect to the baseline had a very small impact on handling qualities. The estimation errors of these parameters are therefore not a critical factor with respect to handling qualities. The methods used to estimate

these parameters are therefore judged to be sufficiently accurate for the application.

The pitch handling quality investigation shows that the swept gull-wing configuration and the Exulans has enough promise to warrant further investigation into its handling qualities. The recommendations for further investigation are outlined in the next section.

Chapter 11

Recommendations

The conclusions from the previous sections pointed out that the Exulans (as an example of a swept gull-wing configuration) should have acceptable longitudinal handling qualities. This section will list topics that were identified during the course of this study that will also have an influence on handling qualities in general.

The following topics for future work were identified:

- The lateral handling characteristics of the gull-wing configuration have to be evaluated. Required roll and yaw rate criteria need to be defined for the Exulans. Control surface sizes must then be evaluated to prove that these criteria can be met. Time domain simulation techniques can be used to evaluate whether roll and yaw rate criteria are satisfied.
- The gull-wing configuration must be analysed with respect to wingtip stall. The tip stall is manifested as a pronounced pitching and rolling instability. The tip stall also usually occurs in the region of the elevons, rendering flight controls ineffective. Tailless aircraft have been known to exhibit tip stall behaviour at low static margins. A detailed *CFD* and wind tunnel study must be performed at different pitch rates to investigate whether this occurs with the gull-wing configuration. The models that are used for the investigation must have low static margin configurations. Flight testing done previously with the SB-13 has shown tip stall problems to develop at low static margin. Fences or

other techniques must then be identified to solve this problem, should it occur.

- Detailed aerodynamic analysis and testing needs to be done to determine whether the shape of the fuselage could be used to prevent tumbling. Past research indicates that thick airfoil sections have a tendency to be less susceptible to tumbling. Engine nacelles, canopies and any protrusions from the aircraft could also have an effect on tumbling. A detailed aerodynamic analysis can possibly yield aerodynamic solutions to prevent the onset of tumbling.
- The pitch stick force gradient of the Exulans was used as 25 N/g for the analyses performed. This stick force gradient was an initial assumption, since the aircraft was not constructed at the time of completion of this study. This gradient must be optimised for the case of the Exulans. The optimised value should then be used as a design input to the gearing of the flight controls of the Exulans.
- A pilot in the loop simulator study should be performed. The work presented in this document eliminated the human pilot as a variable, although a mathematical pilot model was used for one analysis. The effect of the human pilot should now be studied on a pitch flight simulator. This must be done to quantify the effect of the variance of pilot skill on the Exulans handling qualities. The pitch stick force gradient mentioned in the previous point should be used as an input to the simulator study.
- A modal analysis should be performed on the structure of the Exulans. The structure should not have any resonant frequencies that are of same magnitude as that of the human pilot pitch stick input (2-3Hz). The structural resonant frequencies should also be higher than the frequencies of typical gust disturbances. Such a modal analysis can be performed with either a structural ‘bonk’ test or by means of finite element analysis.

- It is anticipated that the Exulans will have degraded handling qualities at speeds above the design airspeed. It is consequently a recommendation that the aircraft should be operated at speeds less than the design airspeed.

The following recommendations can be made with regards the safe expansion of the flight envelope during flight testing of the full-scale Exulans prototype. These recommendations are made based upon the results of the handling quality study:

- Flight testing should commence in calm conditions and at sea level, since gust rejection handling qualities are more favourable for these conditions.
- The static margin for the initial testing phase should be kept between 5% to 7%. The reason for this value is that tip stall is not expected at these values of static margin and handling qualities are expected to be acceptable.
- The landing manoeuvre should preferably be executed by means of a flaring manoeuvre that is achieved with forward wing sweep, as opposed to using elevons to pitch up the nose. This is because excessive use of the elevons increase the risk of the pancaking phenomenon.

